

Copyright Warning & Restrictions

The copyright law of the United States (Title 17, United States Code) governs the making of photocopies or other reproductions of copyrighted material.

Under certain conditions specified in the law, libraries and archives are authorized to furnish a photocopy or other reproduction. One of these specified conditions is that the photocopy or reproduction is not to be “used for any purpose other than private study, scholarship, or research.” If a user makes a request for, or later uses, a photocopy or reproduction for purposes in excess of “fair use” that user may be liable for copyright infringement,

This institution reserves the right to refuse to accept a copying order if, in its judgment, fulfillment of the order would involve violation of copyright law.

Please Note: The author retains the copyright while the New Jersey Institute of Technology reserves the right to distribute this thesis or dissertation

Printing note: If you do not wish to print this page, then select “Pages from: first page # to: last page #” on the print dialog screen

The Van Houten library has removed some of the personal information and all signatures from the approval page and biographical sketches of theses and dissertations in order to protect the identity of NJIT graduates and faculty.

ABSTRACT

Synthesis and Characterization of Silicon Nitride Films Deposited by Plasma Enhanced Chemical Vapor Deposition using Diethylsilane

by
Yanyao Yu

Silicon nitride thin films were deposited on silicon substrates using Diethylsilane (DES) and ammonia by Plasma Enhanced Chemical Vapor Deposition (PECVD) over a temperature range of 100 - 300°C, a pressure range of 0.2 - 0.6 torr, and a ratio of NH₃/DES was varied from 6 - 26. The R.F. power and frequency were kept at 0.15 watts/cm² and 100 KHz respectively. DES flow rate was set at 15 sccm for all experiments in this study. One set of experiments were performed at different values of one parameter while the other parameters were kept constant.

The deposition rate was found to be directly proportional to the chamber pressure, but inversely proportional to the deposition temperature and to the NH₃/DES ratio. The composition of the deposits were determined by ESCA, which found that all films had relatively large concentration of carbon. The carbon content in the films was affected by the reactant ratio, and could be decreased by increasing NH₃/DES ratio. All films as deposited had a compressive stress. Heat-treatment at temperature higher than the deposition temperature lead to a densification of the film and results in films that are less compressive. The increase in NH₃/DES ratio has the effect of increasing the Young's modulus and hardness. This can be explained by saying that the more nitrogen in the film, the higher the Young's modulus.

**SYNTHESIS AND CHARACTERIZATION OF
SILICON NITRIDE FILMS DEPOSITED BY
PLASMA ENHANCED CHEMICAL VAPOR DEPOSITION
USING DIETHYLSILANE**

by
Yanyao Yu

A Thesis
Submitted to the Faculty of
New Jersey Institute of Technology
in Partial Fulfillment of the Requirements for the Degree of
Master of Science in Engineering Science

Committee for the Interdisciplinary Program in
Materials Science and Engineering

October 1993



APPROVAL PAGE

**Synthesis and Characterization of
Silicon Nitride Films Deposited By
Plasma Enhanced Chemical Vapor Deposition
Using Diethylsilane**

Yanyao Yu

Dr. Roland A. Levy, Thesis Advisor
Professor of Physics,
Director of Materials Science and Engineering, NJIT

5/27/93
(Date)

Dr. James M. Grow, Thesis co-Advisor
Associate Professor of Chemistry, NJIT

5/27/93
(Date)

Dr. David, Kristol
Professor of Chemistry,
Graduate Advisor of Biomedical Engineering, NJIT

5/27/93
(Date)

BIOGRAPHICAL SKETCH

Author: Yanyao Yu

Degree: Master of Science in Engineering Science

Date: October 1993

Date of Birth:

Place of Birth:

Undergraduate and Graduate Education:

- Master of Science in Engineering Science,
New Jersey Institute of Technology, Newark, NJ, 1993
- Bachelor of Science in Materials Science,
Shanghai University of Science and Technology, Shanghai, China, 1987

Major: Materials Science and Engineering

ACKNOWLEDGMENT

The author wishes to express his sincere gratitude to his advisors, Professors Roland A. Levy and James M. Grow, for their valuable guidance, encouragement and financial support throughout this research, without which it would not have been completed.

Special thanks are due to Vitaly Sigal for his technical support, valuable suggestions, and friendship during this research work.

The author appreciates the timely help and suggestions from the CVD Laboratory members, including Bozena Szkudlarski, Wei-pin Kuo, Mahalingam Bhaskaran, Wei-Ching Liang, Venkat Paturi, Xianqun Fang and Yan Gao.

TABLE OF CONTENTS

Chapter	Page
1 Review of Si ₃ N ₄ Preparation Methods.....	1
1.1 Various Preparation Methods.....	3
1.2 Comparison of Si ₃ N ₄ Deposited by LPCVD and PECVD.....	16
2 EXPERIMENTAL PROCEDURES.....	17
2.1 Introduction.....	17
2.2 Preparation Work For Experiment.....	18
2.2.1 Leakage Check.....	18
2.2.2 DES Flow Rate Calibration.....	21
2.2.3 Susceptor Temperature Calibration.....	22
2.3 Reactor Etching.....	24
3 EXPERIMENTAL RESULTS.....	26
3.1 Introduction.....	26
3.2 Results and Discussion.....	26
3.2.1 The Effect of Deposition Parameters on Film Properties.....	26
3.2.2 The IR Spectra of Plasma Silicon Nitride Films.....	37
3.2.3 The Effect of Heat Treatment on Film IR and Stress.....	40
3.2.4 Deposition Uniformity of the Film.....	40
3.2.5 Effect of Deposition Time on Deposition Rate.....	43
3.2.6 Optical Transparence Analysis.....	43
3.3 Characterization of Si ₃ N ₄ Films.....	43
3.3.1 Mechanical Stress Measurement.....	43
3.3.2 Hardness and Young's Modulus Measurement.....	46
4 CONCLUSIONS.....	51
APPENDIX A PHYSICAL PROPERTIES OF DIETHYLSILANE (DES).....	52

APPENDIX B THE PRINCIPLE OF THE OPTICAL IMAGING METHOD.....	53
APPENDIX C DEPOSITION PROCEDURE.....	55
REFERENCE.....	57

LIST OF TABLES

Table	Page
1.1 Physical and Chemical Properties of LPCVD and PECVD Si ₃ N ₄	16
2.1 DES Calibration Results.....	23
3.1 Experiment Condition.....	27
3.2 Experiment Results.....	28

LIST OF FIGURES

Figure	Page
1.1 Equipment for depositing Si ₃ N ₄ films by the CVD technique.....	5
1.2 Equipment for depositing Si ₃ N ₄ layers by chemical transport technique.....	7
1.3 A schematic diagram of an ion implantation system.....	8
1.4 A schematic diagram of R.F. reactive sputtering apparatus.....	10
1.5 A schematic diagram of vacuum evaporation equipment.....	11
1.6 PECVD reactor for producing Si ₃ N ₄ films.....	13
2.1 Optical system for stress measurement setup.....	19
2.2 A schematic diagram of the indenting mechanism of the Nano-indenter.....	20
2.3 DES calibration factor as a function of DES flow rate.....	23
2.4 Susceptor temperature calibration.....	25
3.1 Deposition rate as a function of substrate temperature.....	30
3.2 Film density as a function of substrate temperature.....	30
3.3 Refractive index as a function of substrate temperature.....	31
3.4 The surface of the film deposited at 100 C after one month.....	31
3.5 Effect of NH ₃ /DES ratio on deposition rate.....	33
3.6 Effect of NH ₃ /DES ratio on film density.....	33
3.7 Effect of NH ₃ /DES ratio on refractive index.....	34
3.8 Effect of chamber pressure on deposition rate.....	34
3.9 Effect of chamber pressure on film density.....	36
3.10 Effect of chamber pressure on refractive index.....	36
3.11 Infrared spectrum for the plasma deposited silicon nitride film.....	38
3.12 IR spectrum one month after deposition for the film deposited at 100 C.....	39
3.13 IR spectrum of silicon nitride before and after annealing.....	41

3.14 Deposition rate profiles as a function of radial position.....	42
3.15 Effect of deposition time on deposition rate.....	42
3.16 A typical optical transmission diagram.....	44
3.17 Effect of substrate temperature on Young's modulus.....	48
3.18 Effect of substrate temperature on hardness.....	48
3.19 Effect of NH ₃ /DES ratio on Young's modulus.....	49
3.20 Effect of NH ₃ /DES ratio on hardness.....	49
3.21 Effect of NH ₃ /DES ratio on Young's modulus with no N ₂	50
3.22 Effect of NH ₃ /DES ratio on hardness with no N ₂	50
B.1 The principle of the optical imaging method.....	54

CHAPTER 1

REVIEW OF Si₃N₄ PREPARATION METHODS

In recent years, silicon nitride films deposited by low temperature process are still of growing interest to semiconductor industry(1-9). Because silicon nitride films provides a high barrier against moisture and mobile ions e.g. Na⁺, K⁺, etc., and it is hard material, it can be used as final passivation layer and encapsulating material to protect soft aluminum metal lines from scratches and mechanical damage for VLSI(10).

In IC technology, low temperature processes are the most important part of device manufacturing technology to achieve the precise control required for device structure, isolation and interconnection. These have enabled the minimization of undesirable effects like wafer wrapage, Al hillock formation, defect generation, dopant diffusion and Al/Si interface degration(11).

Chemical Vapor Deposition (CVD) is the most common method for the deposition of silicon nitride films. In this process, the reactants are introduced into reaction chamber where the dissociation of the reactants takes place due to high temperatures with deposition of the products on the substrate surface. Accurate control of the reaction temperature, chamber pressure, and reactant ratio is possible by CVD, resulting in high quality films. However, current CVD technology for film growth requires high temperature (above 400⁰C) to activate the reactants. It is seen that the conventional method of depositing final passivation layer at temperature above 400⁰C can cause shallow junction movement, dopant diffusion, hillock formation on Al surface, resulting in reduced quality of the device. Hence it is desirable to deposit silicon nitride films at temperature lower than 400⁰C.

We have chosen Plasma Enhanced Chemical Vapor Deposition, which has the advantage of low deposition temperature over CVD method. This is of particular interest for silicon processing technology. The use of plasma allows to produce reactive radicals at low temperature enabling films to be deposited at low temperature (even at 200°C).

The primary goals of this research were to prepare and characterize silicon nitride thin films deposited by plasma enhanced chemical vapor deposition using diethylsilane (DES). In industry, silane (SiH_4) or dichlorosilane (SiH_2Cl_2) are usually chosen as the sources of silicon for silicon nitride films in the microelectronic technology(12). Silane is known to be hazardous, highly toxic, and pyrophoric. Also, these gases can dissolve and react with the pump oil during the deposition process. To look for a safe and commercially valuable precursor is essential. DES with a chemical formula of $(\text{C}_2\text{H}_5)_2\text{SiH}_2$ is a safer alternate precursor. The physical properties of DES are listed in appendix A. DES is commercially available from Schumacher with a 99% chemical purity.

In addition to its main use as the impervious passivation layer, silicon nitride films also can be used as insulators deposited over aluminium or gold metallization(13), etching masks in multi-level resist structure(4), supporting membranes for X-ray lithography masks(14), coating for gallium arsenide to prevent arsenic evaporating during heat treatment(15), and dielectric and anti-reflection coatings for solar cells and photo-detectors(16,17).

In this thesis, a review of the various deposition methods of silicon nitride film is to be presented. Some of the basic phenomena essential to the understanding of plasma behavior will be reviewed. The results and characterization of silicon nitride film prepared by Plasma Enhanced Chemical Vapor Deposition will be discussed.

1.1 Various Preparation Methods

Because of the high technological importance of silicon nitride in electronics, this material has been intensively studied both experimentally and theoretically in recent years. Among the different methods of synthesis silicon nitride, plasma enhanced chemical vapor deposition (PECVD) is still prepared as a low temperature deposition technique.

In this chapter, a brief review of different methods of Si_3N_4 thin film deposition is presented. The purpose of review is to outline the deposition techniques and there has been no attempt to indicating the best deposition technique. The properties of the silicon nitride film deposited by Low-Pressure Chemical Vapor Deposition (LPCVD), PECVD, etc. are presented.

Si_3N_4 thin film can be generally deposited by the following techniques[18,19]:

- (1) Chemical Vapor Deposition
- (2) Chemical Transport Technique
- (3) Direct Nitridation
- (4) Ion Implantation
- (5) R.F. Cathodic Sputtering
- (6) Vacuum Evaporation
- (7) Photo-Enhanced Chemical Vapor Deposition
- (8) Plasma-Enhanced Chemical Vapor Deposition

(1) Low Pressure Chemical Vapor Deposition

Chemical Vapor deposition is the process of chemically reacting a volatile compound of a material to be deposited, with other gases, to produce a thin film on a suitable substrate. The fundamental mechanisms underlying the LPCVD process can be explained by the following considerations(20). The mass transfer of gases involves their diffusion across a slowly moving boundary layer adjacent to the

substrate surface. The thinner this boundary layer and the higher the gas diffusion rate, the greater the mass transport that results. Surface reaction rates, on the other hand, depend mainly upon reactant concentration and deposition temperature. The thin film growth by chemical vapor deposition has become one of the most important techniques of thin film formation for modern technology. Uniform and adherent layers without defects and impurities are produced with this technique. The equipment used is comparatively cheap and simple. Furthermore, the capability of controllably creating films of widely varying stoichiometry makes CVD unique among deposition techniques. Some disadvantages of the method are the use of toxic, explosive or corrosive gases in many processes and the use of comparatively high temperatures.

A schematic view of low pressure chemical vapor deposition is shown on Figure 1.1. The system for deposition of Si_3N_4 generally contains a gas or volatile liquid source, gas distribution, reaction chamber, heating system, and control system for deposition. The reaction of silicon based compound with ammonia are used to generate thin film, and nitrogen, argon and helium are used as diluent gases. Film properties depend on deposition temperature, reactants used and their purity, ratio of reactants, gas flow rate, chamber pressure, substrate surface preparation, and geometry of deposition chamber.

(2) Chemical Transport Technique

The substance to be deposited (Si_3N_4) with chemical transport technique is reaction transferred by a gaseous reagent (HF or HBr) to produce volatile products. In the region of the substrate (silicon), which is maintained at a higher temperature, the reverse reaction takes place and Si_3N_4 is thus deposited on the silicon[18]. The chemical transport technique offers the advantage of a comparatively high deposition rate for films with controlled composition and purity. The deposition rate

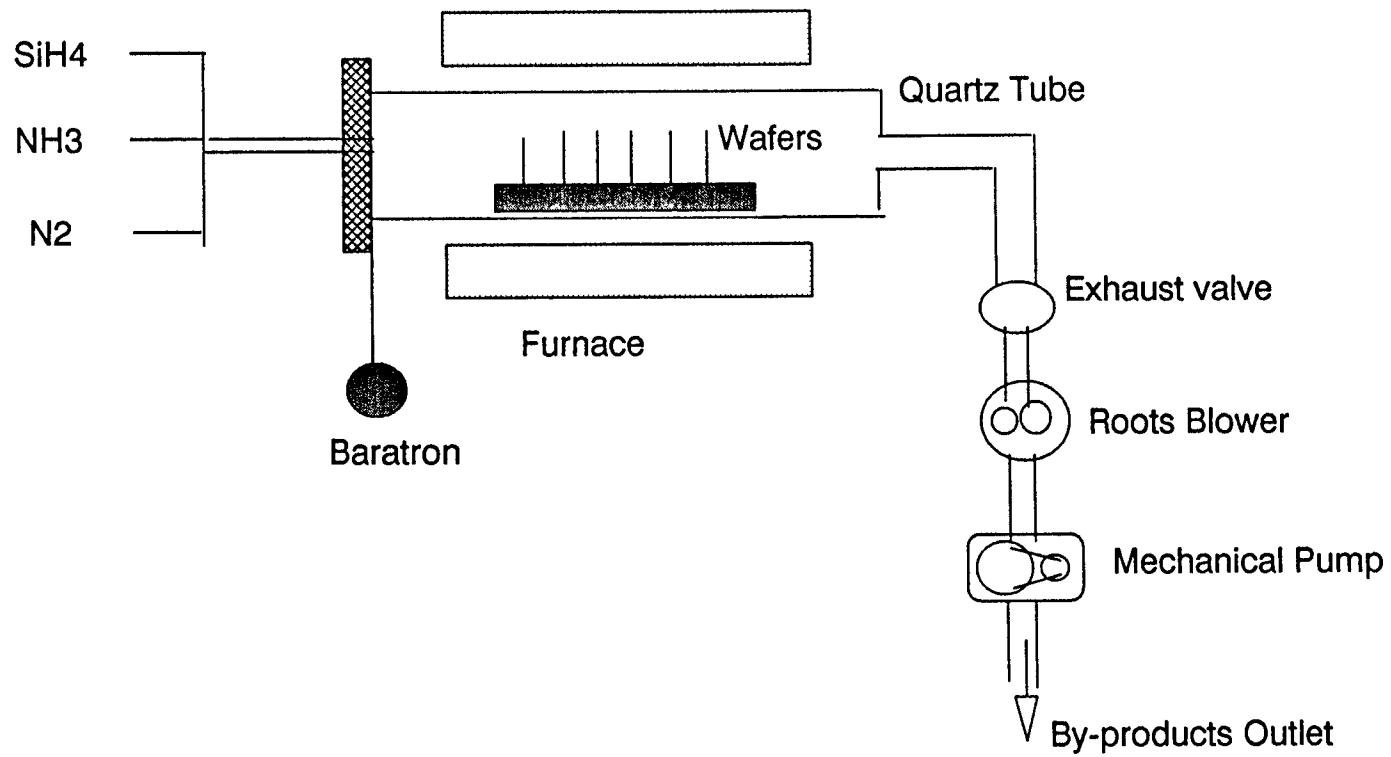


Figure 1.1 Equipment for depositing Si_3N_4 films by the CVD technique.

depends on the temperature of Si_3N_4 source and silicon substrate, and on the concentration of the transport agent. However, the process involves a complex thermochemistry, the kinetics of the chemical reaction are complex and corrosive substances are used. The schematic diagram of equipment is shown on Figure 1.2.

(3) Direct Nitridation

In this technique(21), the experiments occur at temperatures above 900°C , using low nitrogen or ammonia flow rate (1 liter/mm). Silicon directly interacts with nitrogen or ammonia. Film formation rates were very slow (approx. $500 \text{ \AA}/16$ hours) and the growth by direct nitridation is self-limiting. Because of these difficulties, films for commercial applications are not produced by this technique.

(4) Ion Implantation

In this technique(22), a large dose of nitrogen ions are implanted in single-crystal silicon substrates to produce a nitride layer on the surface after annealing. Annealing of the substrates is necessary because of high crystalline damage to the silicon substrate. The properties of the thin films are controlled by the implant voltage, the ion mass, and the ion dose. The ion implantation system(Figure 1.3) includes an ion source, an accelerating column, a vacuum pump, a mass analyzer, a beam scanner, an ion detector and a sample chamber.

(5) R.F. Cathodic Sputtering

Thin layer deposition by cathodic sputtering[19] is based on cathode erosion by bombardment with ionized gas molecules from the discharge enclosure maintained at a vacuum of about 10^{-3} Torr.

A schematic diagram of the cathodic sputtering deposition system is shown on Figure 1.4. Deposition of Si_3N_4 onto silicon substrates are achieved in two ways: by

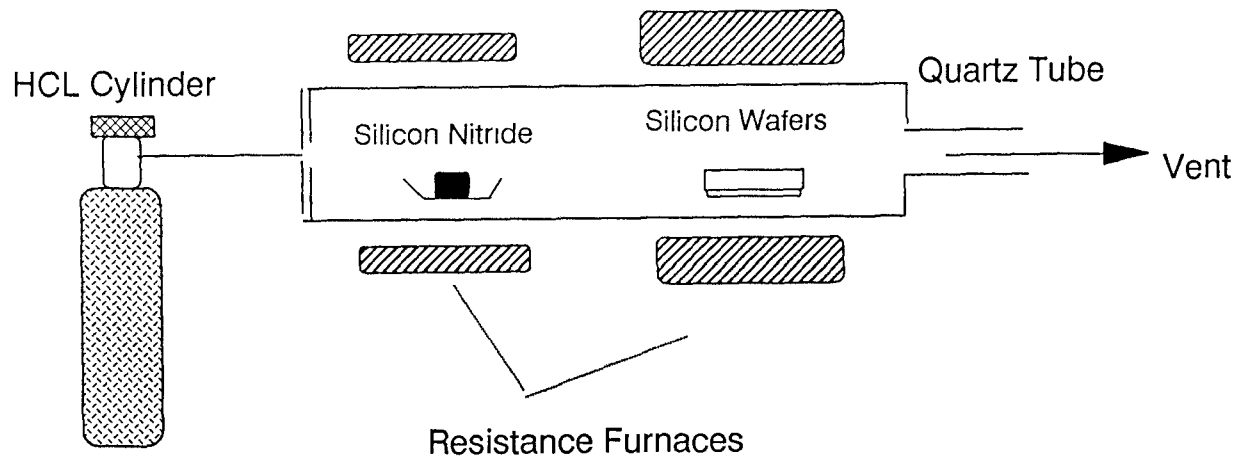
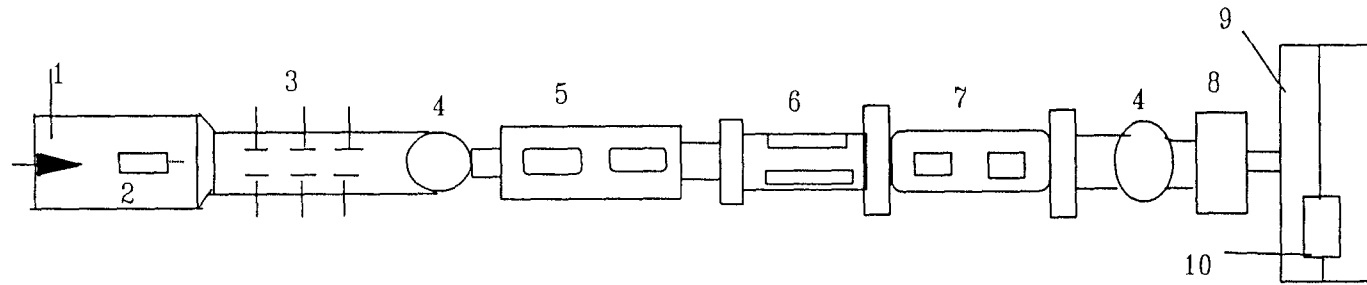


Figure 1.2 Equipment for depositing Si_3N_4 layers by the chemical transport technique.



- | | |
|---|-----------------|
| 1 gaseous source supply (N ₂) | 2 ion source |
| 3 accelerating column | 4 vacuum pumps |
| 5 quadrupole lens | 6 mass analyser |
| 7 beam scanner | 8 ion detector |
| 9 sample chamber | 10 wafer rack |

Figure 1.3 A schematic diagram of an ion implantation system.

direct cathodic sputtering when the material to be sputtered is Si_3N_4 and by reactive cathodic sputtering when silicon is sputtered in N_2 atmosphere. For sputtering in an R. F. plasma the dielectric is first bombarded by positive ions and then by electrons generated by discharge. Ions with high energy will produce atomic(molecular) sputtering of the dielectric; atoms are then deposited onto the substrates and the electrons will prevent the formation above the substrates of a positive space charge which would impede the sputtering process.

The main advantage of this work is low temperature deposition and at same time low mechanical stress are developed between the film and the substrate. However, the film stoichiometry is difficult to control, the film have a low density, and the films show numerous pinholes. The deposition rate depends mainly on R. F. power density and on the argon or N_2 gas pressure.

(6) Vacuum Evaporation

The evaporation method consists of heating the source material (Si_3N_4) with an electron beam at low pressure (10^{-5} Torr) in an evacuated bell jar. The vapors condense as a thin film on all the exposed surfaces of the bell jar including the substrate(18). Room temperature deposition is the advantage of this method, but the films have numerous structural defects. This technique is unsuitable for this aspect of electronics technology (see figure 1.5).

(7) Photo-Enhanced Chemical Vapor Deposition (PHCVD)

This type of process is based on activation of the reactants in the gas or vapor phase by electromagnetic (usually short wave ultraviolet) radiation(23). Selective absorption of photonic energy by the reactant molecules or atoms initiates the process by forming very reactive free radical species that interact to form a desired film product. Typically, Mercury vapor is added to the reactant gas mixture as a

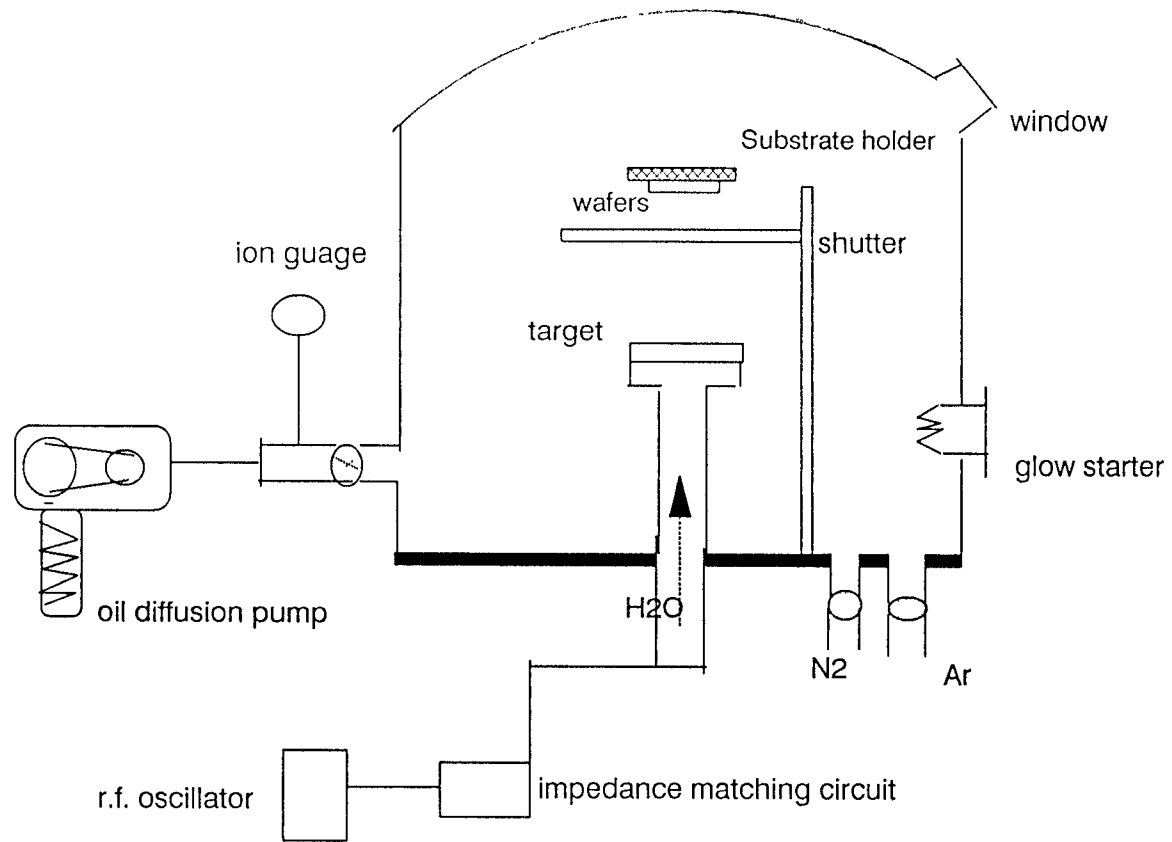


Figure 1.4 A schematic diagram of R.F. reactive sputtering apparatus.

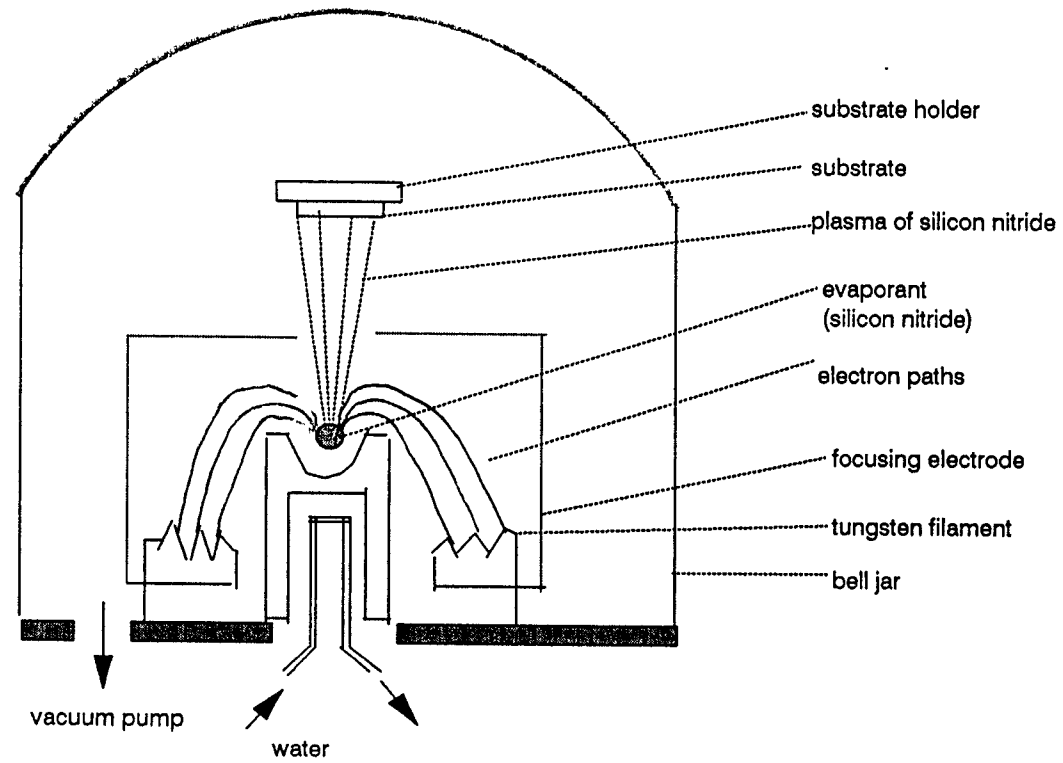


Figure 1.5 A schematic diagram of vacuum evaporation equipment.

photosensitizer and is being activated by the radiation from a high intensity quartz mercury resonance lamp (253.7 nm wavelength). The excited mercury atoms transfer their energy kinetically by collision to reactants to generate free radicals. The advantage of this process is the low temperature (typically 150°C) needed to form films. The limitation at present is the need (in most cases) for photoactivation with mercury to achieve acceptable rates of film deposition. Thus, mercury contamination results. Direct photolysis without the need for mercury can be accomplished in some cases if very intense high energy ultraviolet radiation is used. The reactant gases used in most case for preparation of silicon nitride film are SiH₄ and NH₃. At present, no production reaction reactors available commercially.

(8) Plasma-Enhanced Chemical Vapor Deposition (PECVD)

Figure 1.6 shows the manner in which a glow discharge progresses in a low-pressure gas using a high-impedance power supply(23-25). When a voltage is first applied, a very small current flows due to the small number of initial charge carriers sources (e.g., cosmic radiation) in the system. As the voltage is increased, sufficient energy is imparted to the charged particles to create more charged particles by collisions with the electrons and with neutral gas atoms.

A discharge is essentially a plasma-i.e., a partially ionized gas composed of ions, electrons, and neutral species that is electrically neutral when averaged over all the particles contained within. In Plasma-Enhanced chemical Deposition processing, glow discharge plasma are sustained within chambers where simultaneous CVD reactions occur. The reduced-pressure environment used is somewhat reminiscent of LPCVD systems. Generally, the radio frequencies employed range from about 100 KHz to 40 MHz at gas pressure range from 50 mtorr to 5 torr. Under these conditions, electron and positive-ion densities between 10^9 and 10^{12} /cm³, and average electron energies range from 1 to 10 eV, this energetic discharge

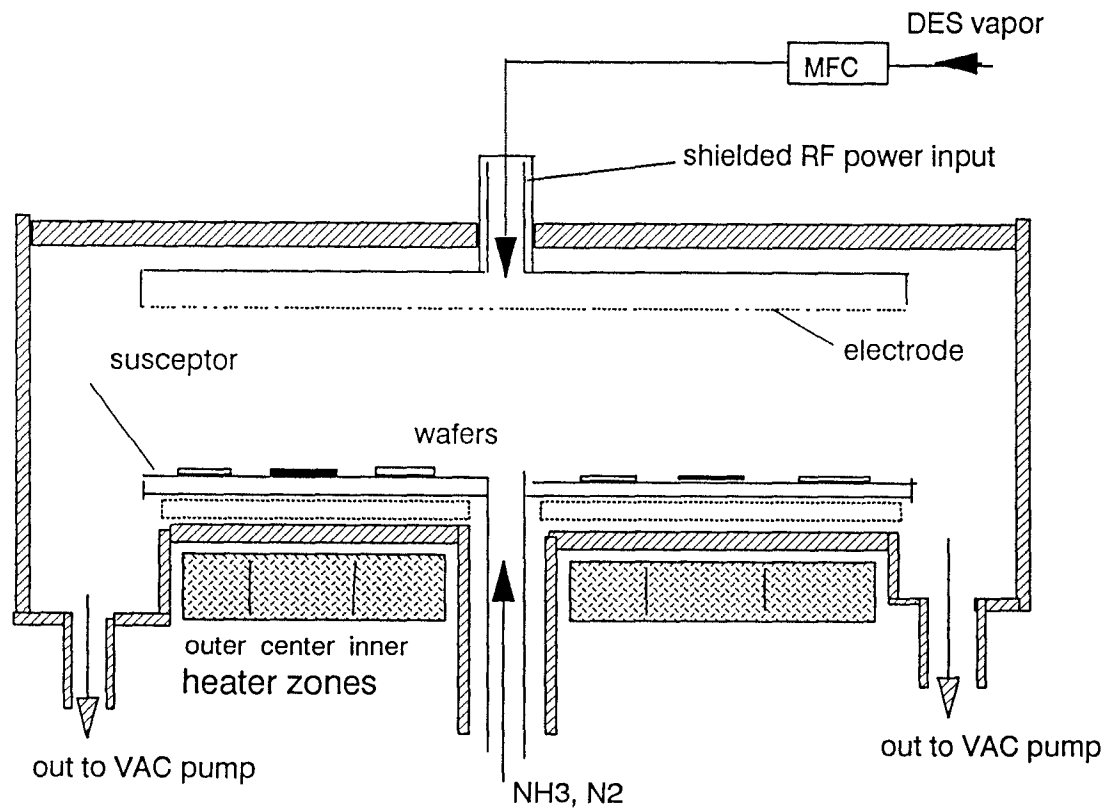


Figure 1.6 PECVD reactor for producing Si₃N₄ films.

environment is sufficient to decompose gas molecules into a variety of component species, such as electrons, ions, atoms, and molecules in ground and excited states, free radicals, etc. By electron impact on relatively stable molecules, active species such as ions, excited molecules, and radicals are formed. In a low pressure plasma (total pressure around 100 Pa), the mean electron energy is around 2 eV, while the electron concentration and the positive ions are about 10^{10} cm^{-3} . The electron density is determined by the mean electron energy, the electric field, the geometry of the system, the gas species, and the total pressure. Furthermore, the electron density is determined by the balance between the generation rate and the loss rate of electrons. Ionization is the most important process in sustaining the plasma, while electrons are lost by diffusion and recombination at surface. Drevillion et. al. determined (26), at pressure around 100 Pa the concentration of ions is two to three orders of magnitude smaller than the free radical concentration. The formed radical may react by conventional pathways, but chemical reactions at surface can also be enhanced by processes such as ion bombardment. The bombarding energy depends on the difference between the plasma potential and the substrate potential, the total pressure and the frequency of the applied field(27). At low frequency, ions and electrons can follow the alternating R.F. field, therefore ion impingement can take place on the growing layer. Ions which leave the plasma are accelerated in the dark space and acquire a maximum energy of $V_p - V_s$ (V_p is the plasma potential and V_s is the substrate potential), when they reach the substrate. In reality, collision take place in the dark space, therefore, the bombarding energy decrease with increasing total pressure.

The net effect of the interactions among these reactive molecular fragments is to cause chemical reactions to occur at much lower temperature than in conventional CVD reactors without benefit of plasma. The uniqueness of plasma to generate chemically reactive species at low temperature is due to the nonequilibrium nature

of the plasma state. By nonequilibrium, we mean a gas plasma sustained at low pressure, which exhibits temperatures of the free electrons of tens of thousands of degrees Kelvin, while the temperature of the translational and rotational modes of free atoms, radicals, or molecules will be only hundreds of degrees Kelvin. Therefore, previously unfeasible high-temperature reaction can be made to occur on temperature-sensitive substrates. The films that deposited by plasma reaction are usually amorphous in nature, with very little short range structure ordering. The stoichiometry of the films can be made to vary by controlled variation of important plasma parameters, such as reactant gas flow ratios. Redeposition of the material due to ion bombardment during plasma deposition is possible to improve step coverage of the film. During PECVD processing, the discharge is excited due to the fact that Si_3N_4 film is dielectric, and a dc discharge is not feasible.

In a glow discharge, the rate of dissociation processes can be described by (28) $R = K_d[e][X]$, where $[e]$ and $[X]$ are the mean concentration of electrons and monomers, respectively, and K_d is the rate constant for dissociation. This constant depends on the average electron energy, the shape of the electron distribution function, and the cross section of the different species. As the mean electron energy or electron temperature is much higher than the substrate temperature, it can be concluded that the electron impact dissociation rate is nearly independent of the deposition temperature. However, in the pressure regime under discussion, the rate coefficient for ionization is at least two orders of magnitude smaller than the rate coefficient for dissociation.

A major commercial application of PECVD processing has been to deposit silicon nitride films in order to passivate and encapsulate completely fabricated microelectronic devices. A parallel plate plasma deposition reactor is commonly used for Si_3N_4 deposition. Several production reactors are commercially available.

1.2 Comparison of Si₃N₄ Deposited by LPCVD and PECVD

Si₃N₄ films deposited by different preparation techniques are discussed above. A physical and chemical properties comparison between LPCVD and PECVD are shown in table form (table 1.1). The result in the table is compiled from the literature.

Table 1.1 Physical and Chemical Properties of LPCVD and PECVD Si₃N₄

	High temp. nitride	Plasma dep. nitride
Property	900°C	300°C
composition	Si ₃ N ₄	Si Nx
Si/N	0.75	0.8 - 1.0
Solution Etch Rate		
Buffered HF (25°C-25°C)	10 - 15 A/min	200 - 300 A/min
Plasma Etch Rate		
92% CF ₄ - 8% O ₂ , 700W	600 A/min	1000 A/min
Na+ penetration	<100 A	<100 A
IR Absorption		
Si - N max	~ 830 cm ⁻¹	~830 cm ⁻¹
Si - H minor	---	2,200 cm-1
Density	2.8 - 3.1 g/cm ³	2.5 - 2.8 g/cm ³
Refractive Index	2.0 - 2.1	2.0 - 2.1
Dielectric constant	6 - 7	6 - 9
Dielectric strength	1 x 10 ⁷ V/cm	6 x 10 ⁶ V/cm
Bulk Resistivity	10 ¹⁵ - 10 ¹⁷ ohm-cm	10 ¹⁵ ohm-cm
Surface Resistvity	>10 ¹³ ohm/sq	1 x 10 ¹³ ohm/sq
Intrinsic Stress	1.2 - 1.8 x 10 ¹⁰ dyn/cm ²	1 - 8 x 10 ⁹ dyn/cm ²
	Tensile	Compressive
Thermal Expermal	4 x 10 ⁻⁶ /°C	---
Color, Transmitted	None	Yellow
Step Coverage	Good	Conformal
H ₂ O Permeability	Zero	Low - None

CHAPTER 2

EXPERIMENTAL PROCEDURES

2.1 Introduction

Silicon nitride thin films were deposited in the applied Materials AMP 3300 IIA PECVD system with external DES flow equipment. The scheme is given in figure 1.6. The reaction chamber is an aluminum cylinder with aluminum plates on the top (upper electrode) and the bottom (susceptor). There are 2 inches between upper electrode and susceptor, and about 26 inches for the electrode diameter. There are three resistance heater rings which divided the susceptor into three zones: inner, center and outer zones.

Single crystal silicon wafers (P-type, 10 cm in diameter, 525 μm thick) and plain glass slide (3" x 1" size, 1.1 mm thick) were placed separately in the outer zone of the susceptor (figure 1.6). In order to have an uniform substrate temperature within outer zone, heating of the susceptor for an hour before deposition is necessary. Four wafers and one glass slide were used for each experiment. The mass of deposit was accurately measured to within 0.2 mg by weighing the wafers before and after deposition. Samples were cooled to below 70⁰C in the vacuum environment for about five hours before being removed from chamber. This is done to avoid problems with films that are sensitive to air.

The refractive index of films were measured using a Rudolph ellipsometer, which contains a He-Ne laser (6238 Å wavelength). The film thickness was measured using a Nanometrics NanoSpec/AFT nanospectrometer by inputting refractive index value. The film density was determined using the measured mass and film thickness. The Infrared spectra were taken using a Perkin Elmer 580 IR Spectrophotometer to determined the vibration modes presented in the films. The

optical transmission of films were inspected by DMS 300 UV/visible Spectrophotometer.

The mechanical property of the film stress were measured by home-build optically laser-beam equipment that measured changes in the radius of curvature of a wafer resulting from deposition on a single side. The stress was determined by the wafer (orientation $\langle 100 \rangle$) radius of curvature change between before deposition and after deposition. Figure 2.1 is a optical imaging system for setup. Two circular spots were produced from the two laser beams and were projected on substrate/film by a mirror, then the reflection from the surface of the wafer was projected again on the screen with scale by the mirror. The distance of the two spots on the screen reflected from the mirror was recorded before and after deposition.

The hardness and Young's modulus of the films were determined using a Nano Instruments indenter. Schematic diagram of the indenting mechanism of the Nano-indenter is given in figure 2.2. The indenter is a triangular pyramid-shaped diamond with same area to depth ratio as the traditional wickers pyramid. The position of the indenter is determined by a capacitance displacement gauge. A coil and magnet assembly located at the top of the loading column is used to drive the indenter toward the sample. The force imposed on the column is controlled by varying the current in the coil. The loading column is suspend by flexible springs. A plot of load (mN) vs. displacement (nm) for silicon nitride sample can be obtained from Nanoindentor.

2.2 Preparation Work for Experiments

2.2.1 Periodic leak checking

A leak in the vacuum system will introduce impurities such as oxygen into the reaction chamber during deposition and can change properties of the films. The

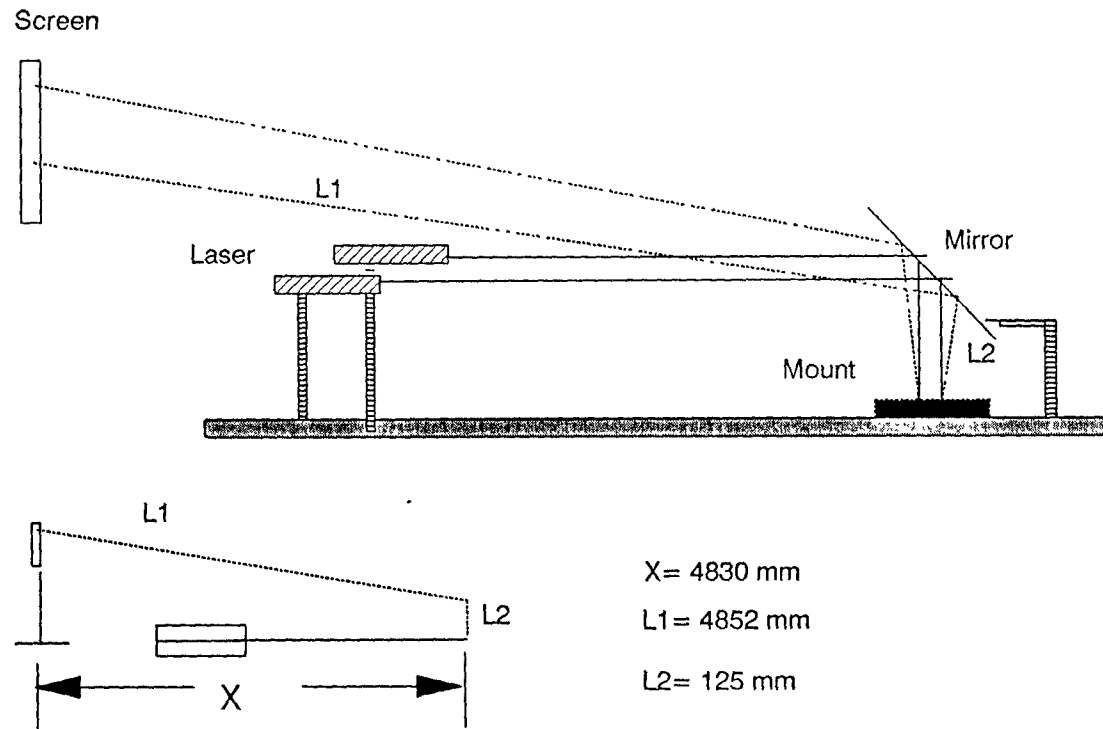


Figure 2.1 Optical system for stress measurement setup.

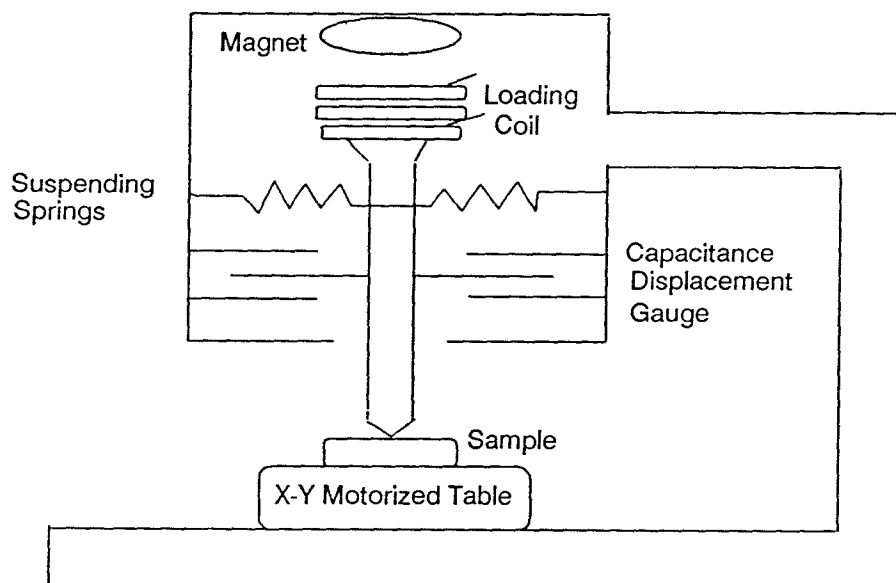


Figure 2.2 A schematic diagram of the indenting mechanism of the Nano-indenter.

system to have leakage check periodically to keep normal deposition condition. Because of system design factor, the leakage was carried out at automatic fillback step without delivering any gases into chamber. At fillback step, only the pneumatic valve for nitrogen gas is open. When carrying out leakage check, the mass flow controller for DES and gas regulators should be open. After pumping the reaction chamber to a low vacuum level, the system was set at fill-back step under manual control mode for 12 hours. The leakage rate was determined by chamber pressure increase 12 hours later. The Applied Materials company recommends the leakage rate should be lower than 10 milli-torr for AMP-3300 IIA PECVD system. For this system, the leakage rate was 3.42 mTorr/min.

2.2.2 DES flow rate calibration

An AFC 550 Automatic Flow Controller manufactured by the Applied Materials company (rang: 20 sccm - 1000 sccm) was used to control DES flow rate in this experiment. To calibrate the automatic flow controller was essential before it was used for controlling DES flow. First, after plumbing and wiring have been completed, to make two adjustments to the AFC is necessary. They are the setpoint calibration and the zero adjustment. Apply power to the AFC for at least one hour before these adjustments. Details of the work is explained in the AFC 550 user's manual. Second, AFC-550 nitrogen calibration was carried out at an other LPCVD system (18.5 litter chamber volume) with a manual valve and manual reactant feeding system. Delivering nitrogen gas into chamber for a certain time result chamber pressure increase. By using the ideal gas law, $PV = nRT$, the following formula was developed to calibrate the flow rate:

$$\frac{dv}{dt} = \frac{V_r}{760} \times \frac{273}{T_m} \times \frac{dp}{dt}$$

Where dv/dt is the flow rate of the tested gas in unit of sccm, V_r is the volume of reactor chamber, T_m is the chamber temperature, dp/dt is the rate of pressure increase. The reactor chamber was evacuated for several hours prior to doing calibration. After setting the flow rate, gas line was opened to introduce the nitrogen flow into chamber, then the outlet manual valve was closed and the pressure difference in the chamber was measured to obtain the rate of pressure increase. Thus, the real flow rate of the tested gas can be calculated from formula above. For this AFC 550 model flow controller used in this study there was only one sccm difference at flow rate of less than 80 sccm between readout flow rate and calibration flow rate.

After the flow controller was calibrated, the DES flow rate was calibrated by same means by delivering DES vapor into chamber. The vapor pressure of DES is about 200 torr at 20°C, while can meet AFC 550 model requirement which needs at least pressure drop of 20 PSI. The factor for DES is defined as the ratio of the real flow rate of DES to the nitrogen flow rate. The Applied Materials company suggests that the flow rate factors of the nitrogen mass flow controller as AFC 550 model, for ammonia, oxygen, Freon are 0.790, 0.986, 0.475 respectively.

The DES calibration results are listed in the table 2.1. The plot of the factors vs. DES flow rate is shown in figure 2.3. The factor is a nonlinear function of DES flow rate. At the range of the flow rate in this study, the factor for DES was calculated to be 0.191.

2.2.3 Susceptor temperature calibration

To know temperature of the susceptor (see figure 1.6) as deposition temperature is essential before the experiments start. The susceptor is heated through conduction from heater, thus set temperature and susceptor temperature must be different. Since high susceptor temperature may cause aluminum parts in the chamber to be

Table 2.1 DES Calibration Results

Set point	readout	DES flow rate	Factor
103	100	19.1	0.191
128	125	23.1	0.185
154	150	27.3	0.182
180	175	32.0	0.183
205	200	36.3	0.182
231	225	40.0	0.178
257	250	44.4	0.178
410	400	70.5	0.176

**Figure 2.3 DES calibration factor as a function of DES flow rate.**

damaged, cooling water must be on before the heater is turned on. For the safety reason, the setting temperature was raised slowly from low point (50⁰C) to high point (400⁰C). It is necessary to wait for one hour to equilibrate susceptor temperature when susceptor temperature was raised up to next setting temperature. The temperature on the top of the susceptor at each zone was measured by a type J thermocouple with chamber door open. Due to heater zone radius difference, inner zone has one heater elements, center zone has three heater elements and outer zone has two heater elements. The temperature difference between inner zone and outer zone was measured to be less than 4⁰C when the heaters were set at the same temperature. Within outer zone, the maximum temperature difference was measured to be 3⁰C. Thus, there is temperature uniformity in the outer zone. The Figure 2.4 shows the plot of susceptor temperature vs. setting temperature. The relation between the susceptor temperature and the setting temperature may be considered as a linear function of $Y = -7.4 + 0.628 * X$, in which Y is the susceptor temperature and X is the setting temperature.

2.3 Reactor Etching

As suggested by Applied Materials AMP - 3300 IIA PECVD system user's manual, the chamber clean condition is considered a variable of deposition. The deposition rate was influenced by chamber clean mess. Thus, to keep same chamber clean condition before each deposition is necessary. This can avoid the peeling of the film deposited on upper electrode in the next experiment. The chamber etching experiment is performed under following condition: the etch mode on engineering control panel must be selected and cooling water must be on before the experiment, the plasma power = 800 W (0.24 watts/cm² power density), the radio frequency = 100 KHz, the chamber pressure = 0.3 torr, the oxygen flow rate = 200 sccm, the

Freon with 8% oxygen flow rate = 300 sccm. The etching time was kept at 45 minutes, and the susceptor heater was off.

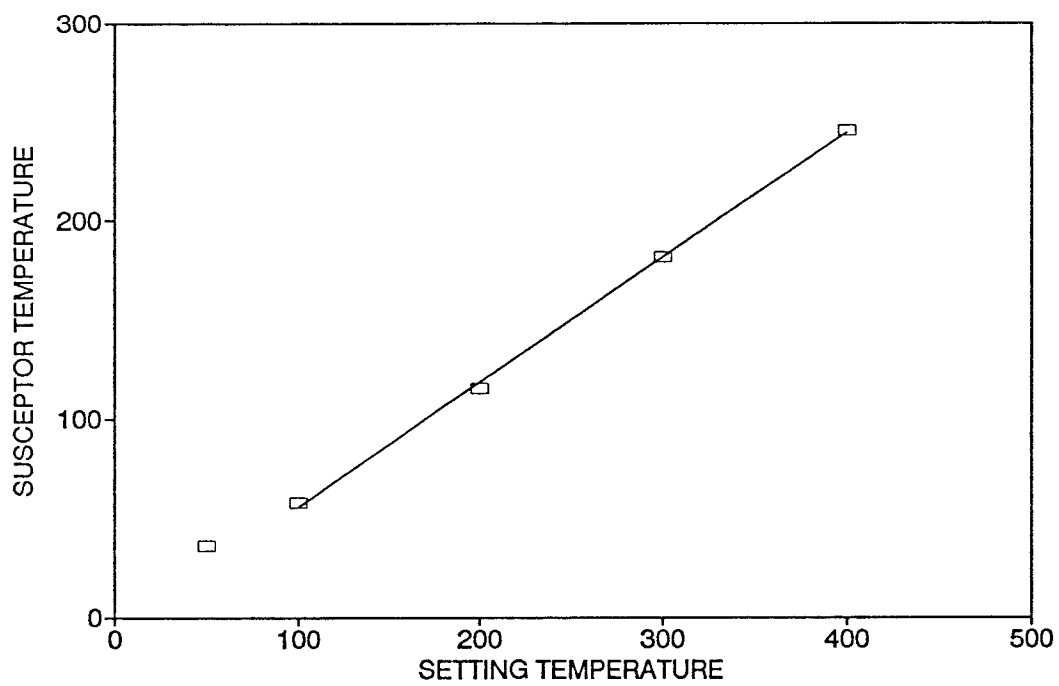


Figure 2.4 Susceptor temperature calibration.

CHAPTER 3

EXPERIMENTAL RESULTS

3.1 Introduction

The properties of plasma silicon nitride layers will be influenced by the deposition parameters such as deposition temperature, gas phase composition, chamber pressure and plasma power density and frequency. One set of experiments were performed at different values of one parameter while the other parameters were kept at constant. In this study, the plasma silicon nitride films were deposited at the temperature range of 100^oC to 300^oC. The chamber pressure was varied from 0.2 to 0.6 torr, and the reactant ratio of NH₃/DES from 6 to 22 with constant total flow rate (345 sccm) and from 10 to 26 with no N₂ (total flow rate varied by NH₃/DES ratio). The flow rate of DES was fixed at 15 sccm for all experiments in this study. The deposition time was set at 45 minutes in order to obtain accurate deposition rate. The experiments in this study were divided into four sets: temperature set, NH₃/DES ratio set with N₂, pressure set, and NH₃/DES ratio set without N₂. The *experimental* experiment conditions are listed in table 3.1. Table 3.2 shows the *experimental* experiments results including deposition rate, film density, refractive index, stress, composition, Young's modulus and hardness.

3.2 Results and Discussion

3.2.1 The Effect of Deposition Variable on Film Properties.

The deposition rate, the film density and refractive index vs. the susceptor temperature are plotted on Figure 3.1 - 3.3. The following deposition condition were used: substrate temperature = 100^oC - 300^oC , the ratio of NH₃/DES = 18, N₂ flow rate = 60 sccm, and chamber pressure = 0.3 Torr. As substrate temperature increases from 100^oC to 300^oC, the deposition rate decreases from 220 Å/min to

Table 3.1 Experimental Condition*

Temperature Study

Temp. (°C)	Sample	Ratio (NH ₃ /DES)	Pressure (torr)	DES	NH ₃ (sccm)	N ₂
100	X06	18	0.3	15	270	60
150	X04	18	0.3	15	270	60
200	X03	18	0.3	15	270	60
250	X02	18	0.3	15	270	60
300	X01	18	0.3	15	270	60

Ratio Study (Total flow rate 345 sccm)

Temp. (°C)	Sample	Ratio (NH ₃ /DES)	Pressure (torr)	DES	NH ₃ (sccm)	N ₂
250	X09	6	0.3	15	90	240
250	X11	10	0.3	15	150	180
250	X10	14	0.3	15	210	120
250	X02	18	0.3	15	270	60
250	X12	22	0.3	15	330	0

Pressure Study

Temp. (°C)	Sample	Ratio (NH ₃ /DES)	Pressure (torr)	DES	NH ₃ (sccm)	N ₂
250	X14	18	0.2	15	270	60
250	X02	18	0.3	15	270	60
250	XA18	18	0.4	15	270	60
250	X18	18	0.5	15	270	60
250	X13	18	0.6	15	270	60

Ratio Study (Total flow rate varied, No N₂)

Temp. (°C)	Sample	Ratio (NH ₃ /DES)	Pressure (torr)	DES	NH ₃ (sccm)	N ₂
250	X23	10	0.3	15	150	0
250	XA21	14	0.3	15	210	0
250	X20	18	0.3	15	270	0
250	X12	22	0.3	15	330	0
250	X22	26	0.3	15	390	0

* at constant R.F. power (500w) and frequency (100 KHz)

Table 3.2 Experimental Results

Temperature Study											
Temp. (°C)	Sample	Deposition rate (Å/min)	Density (g/cm ³)	R. I.*	Stress** (MPa)	Young's modulus	Hardness (GPa)	Composition			
								Si	N	C	O
100	X06	220	1.53		-100	41.4	1.18	27	3	8	61
150	X04	175	1.77	1.72	-110	64.9	2.44	25	5	11	57
200	X03	157	1.84	1.74	-141	87.4	7.37	38	33	23	6
250	X02	129	2.04	1.78	-311	91.3	8.47	37	36	20	7
300	X01	114	2.13	1.80	-467	98.3	9.32	38	34	21	7

Ratio Study (Total flow rate 345 sccm)											
Temp. (°C)	Sample	Deposition rate (Å/min)	Density (g/cm ³)	R. I.	Stress (MPa)	Young's modulus	Hardness (GPa)	Composition			
								Si	N	C	O
250	X09	190	1.84	1.89	-200	77.9	7.51	32	30	31	6
250	X11	169	1.91	1.80	-180	83.4	7.39	36	30	25	8
250	X10	154	1.95	1.79	-228	88.4	7.81	39	31	25	5
250	X02	129	2.04	1.78	-311	91.3	8.47	37	36	20	7
250	X12	127	2.03	1.78	-259	92.8	8.33	34	33	27	6

Table 3.2 Experimental Results (Continued)

Pressure Study											
Temp. (°C)	Sample	Deposition rate (Å/min)	Density (g/cm ³)	R. I.	Stress (MPa)	Young's modulus	Hardness (GPa)	Composition			
								Si	N	C	O
250	X14	121	2.11	1.83	-349			37	37	21	5
250	X02	129	2.04	1.78	-311			37	36	20	7
250	XA18	131	1.98	1.75	-396			33	40	21	6
250	X18	142	1.97	1.75	-410			37	34	24	5
250	X13	156	1.91	1.77	-645			37	34	21	7

Ratio Study (Total flow rate varied, No N ₂)											
Temp. (°C)	Sample	Deposition rate (Å/min)	Density (g/cm ³)	R. I.	Stress (MPa)	Young's modulus	Hardness (GPa)	Composition			
								Si	N	C	O
250	X23	150	1.91	1.82	-171	72.7	7.01	30	27	36	7
250	XA21	126	2.05	1.83	-332	98.3	8.73	34	33	29	4
250	X20	129	2.05	1.80	-266	112.8	10.49	40	33	24	4
250	X12	127	2.03	1.78	-259	92.8	8.33	34	33	27	6
250	X22	113	2.07	1.79	-438	108.8	9.71	39	30	24	6

* at wavelength of 632.8 nm

** - is compressive.

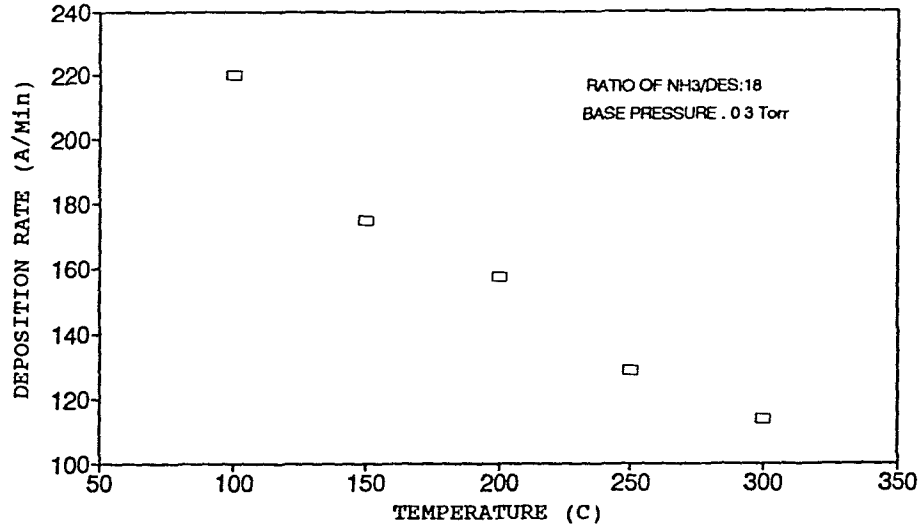


Figure 3.1 Deposition rate as a function of substrate temperature.

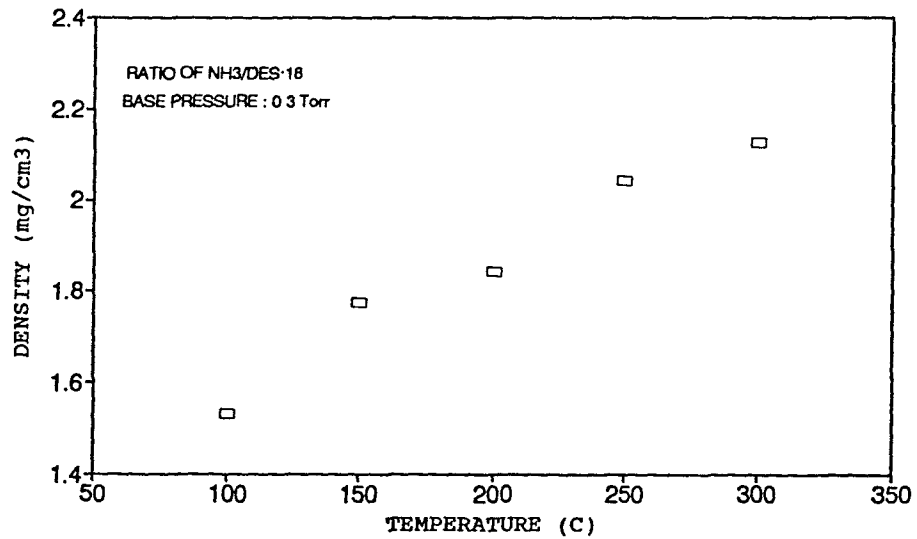


Figure 3.2 Film density as a function of substrate temperature.

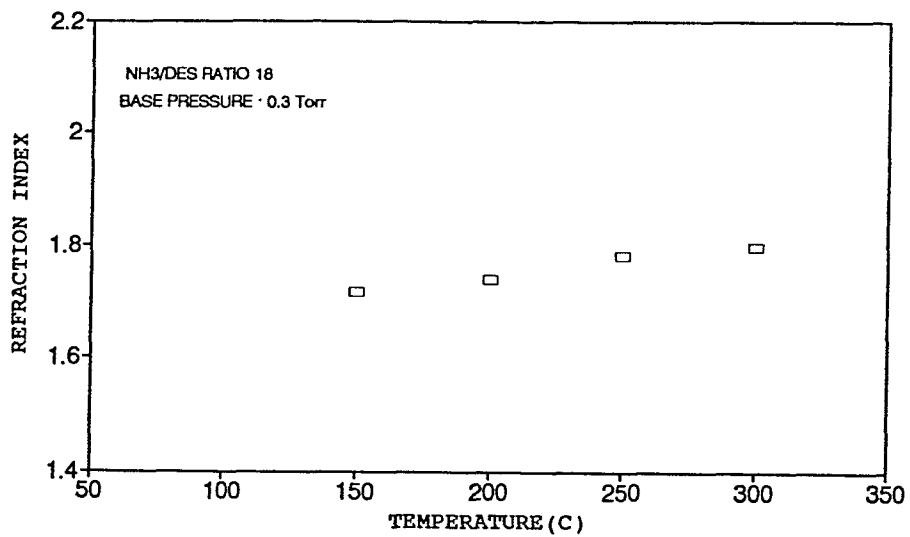


Figure 3.3 Refractive index as a function of substrate temperature.

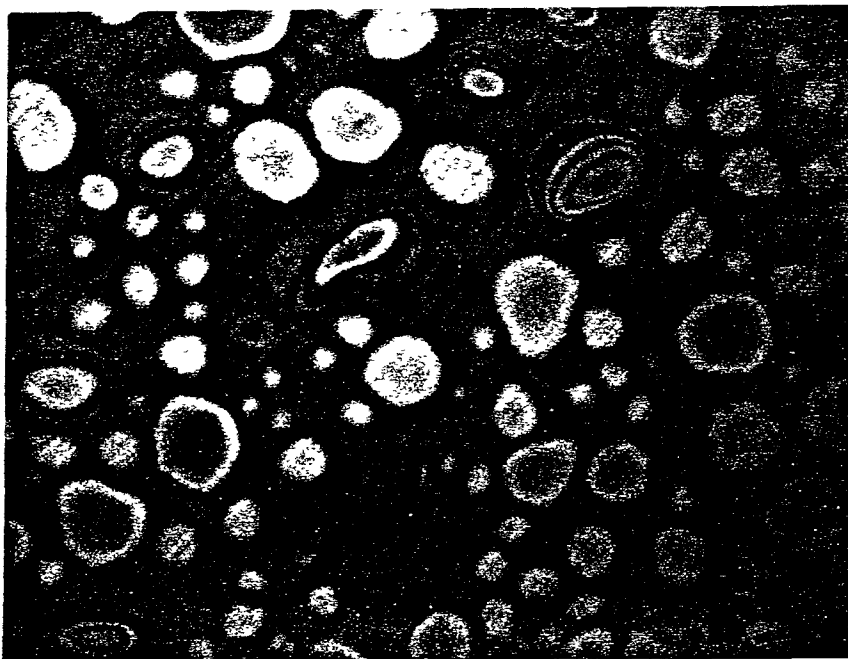


Figure 3.4 The surface of the film deposited at 100 C after one month.

114 Å/min while film density increases. The similar result that deposition rate decreases with temperature was observed in plasma silicon nitride using silane as precursor(25). The composition analysis results by ESCA done by Olin Hunt (table 3.2) shows carbon concentration increase slightly as substrate temperature increase. This can be explained by that DES is a source of carbon and deposited at relatively high substrate temperature. The increase in refractive index with temperature was also observed by other researcher(2), and related to Si/N and C/N ratio.

One thing worth to note is that the film deposited at 100°C was chemically unstable and found to change in surface color after exposed to the air for one and half months. IR Spectra of plasma silicon nitride film deposited at 100°C showed Si-N bonding did not exist 1.5 months after deposition, instead, a Si-O bonding appeared. Figure 3.4 shows the surface of the film deposited at 100°C after 1.5 months.

In figure 3.5 - 3.7, the ammonia concentration was changed by varying the input gases NH₃ and N₂ while the DES flow rate was kept constant. The total flow rate was kept at 345 sccm. In this set of experiments, the increase of NH₃/DES ratio resulted in a decrease in the deposition rate and in an increase in the films density. The refractive index does not varied significantly with the reactant ratio. The carbon concentration is also influenced by NH₃/DES ratio. The ESCA analysis showed that the carbon concentration decreased as the reactant ratio of NH₃/DES increased. The Si/N ratio of the deposited layers is only varied with increasing ammonia flow rate. The film density increased as function of the NH₃/DES ratio as shown in figure 3.6. In the ratio set experiments without nitrogen gas, the ESCA analysis also shows the carbon concentration decreased as reactant ratio of NH₃/DES increased and the carbon was present more as free carbon than in the other three sets. The ratio of the free carbon/carbide was in the range between 55/45 to 60/40 for the ratio set experiments without nitrogen gas.

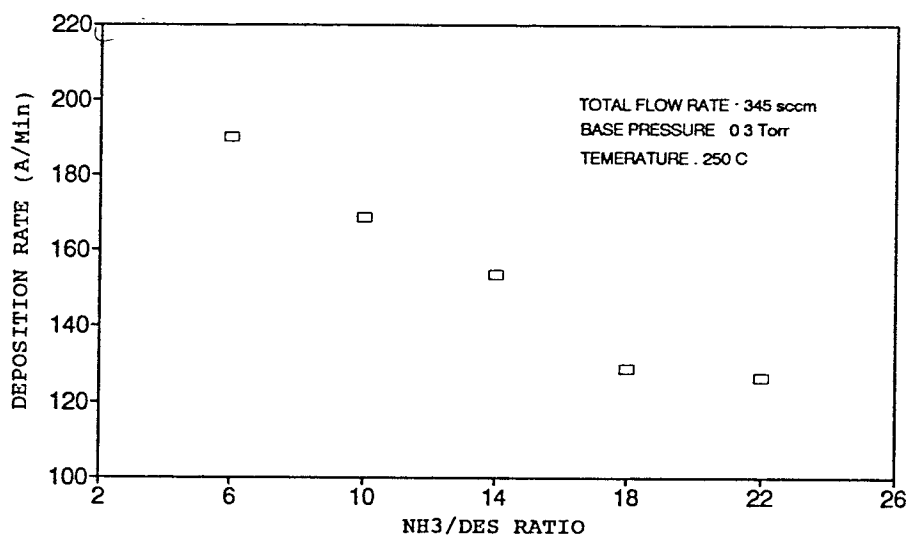


Figure 3.5 Effect of NH₃/DES ratio on deposition rate.

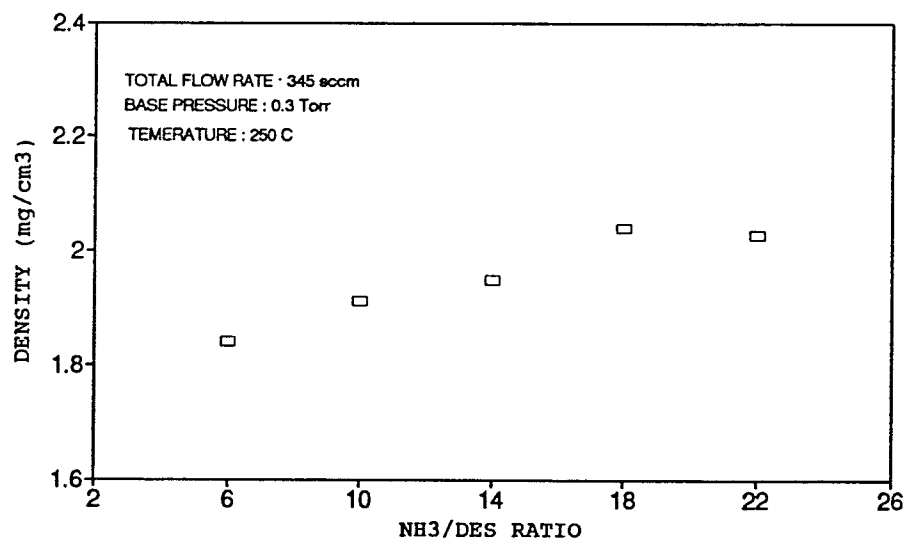


Figure 3.6 Effect of NH₃/DES ratio on film density.

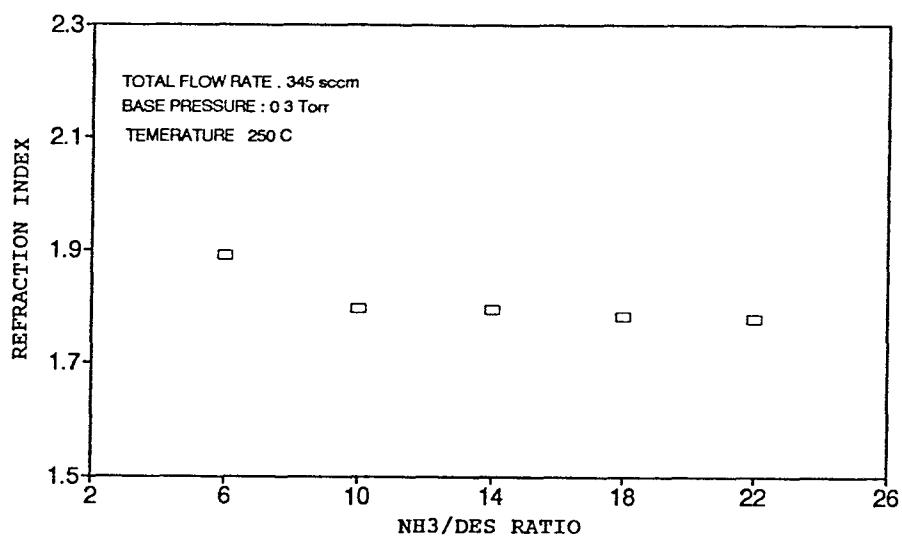


Figure 3.7 Effect of NH₃/DES ratio on refractive index.

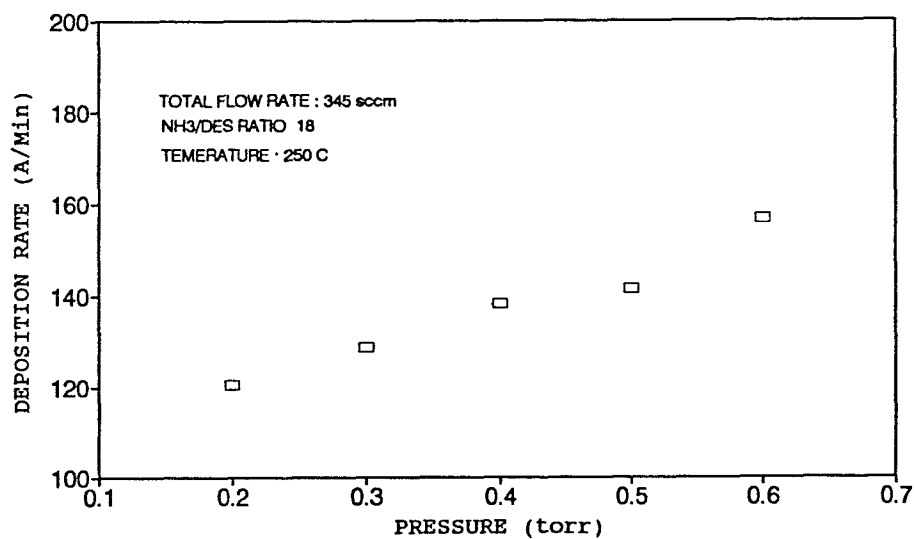


Figure 3.8 Effect of chamber pressure on deposition rate.

At constant NH_3/DES ratio and total flow rate, change in chamber pressure affected the deposition rate. As seen in figure 3.8 where the chamber pressure as a function of the deposition rate can be seen, the deposition rate increased as the chamber pressure increased. The deposition rate increased from 121 Å/minute to 156 Å/minute, when the chamber pressure was increased from 0.2 Torr to 0.6 Torr. Thus, a three fold increase in the chamber pressure increased the deposition rate significantly. When the chamber pressure increased at constant R.F. power, the film density decreased (figure 3.9). The refractive index was not affected by chamber pressure at range of 0.3 torr to 0.6 torr as shown in figure 3.10. The same result is reported by other investigator with the $\text{SiH}_4\text{-NH}_3\text{-N}_2(2)$.

A brief review of some characteristic of a glow discharge which are typical for a plasma deposition system has been given in chapter 1. The deposition rate of plasma silicon nitride using DES depends on deposition temperature, reactant ratio, and chamber pressure as shown in figure 3.1 - 3.10. In a glow discharge, the rate of ionization can be described by expression $R = K_d[e][X]$. Based on discussion in the results obtained by Blaluw(2), the deposition rate vs. the deposition temperature (figure 3.1) can be explained by the decrease in hydrogen content of films deposited at higher temperature leading to the deposition rate decrease. The ratio of Si/N of the films deposited at 200°C - 300°C did not change, but the deposition rate reduced from 157 Å/min to 114 Å/min. During deposition at low temperature, more hydrogen is captured and can not escape from surface layer by thermal diffusion. Rich hydrogen content reduces the density of the film significantly. Thus, the increase of the deposition temperature decrease the deposition rate, leading to a film density increase.

Increasing the NH_3/DES ratio in the gas mixture decreased the Si/N ratio in the deposition films has been established(29). This can be ascribed to the higher dissociation energy of N_2 compare to that of NH_3 . For our study, the ESCA analysis

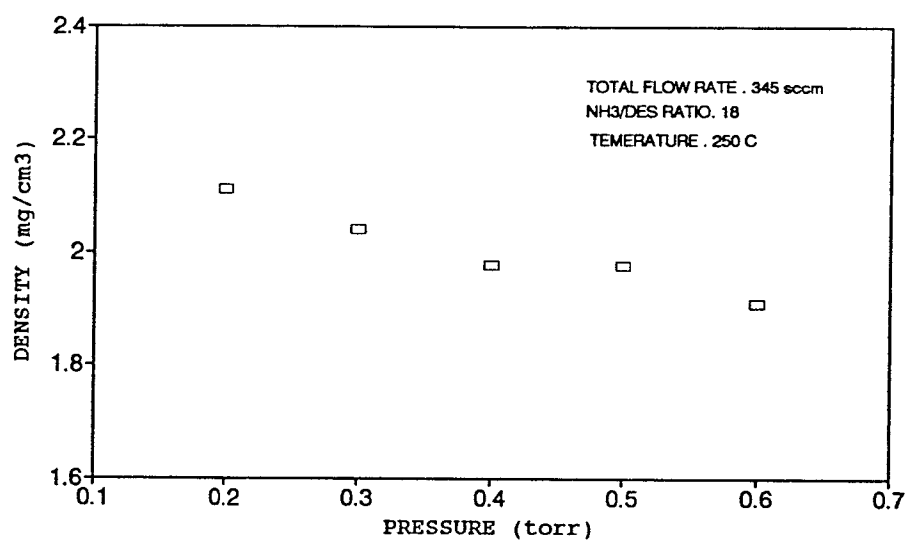


Figure 3.9 Effect of chamber pressure on film density.

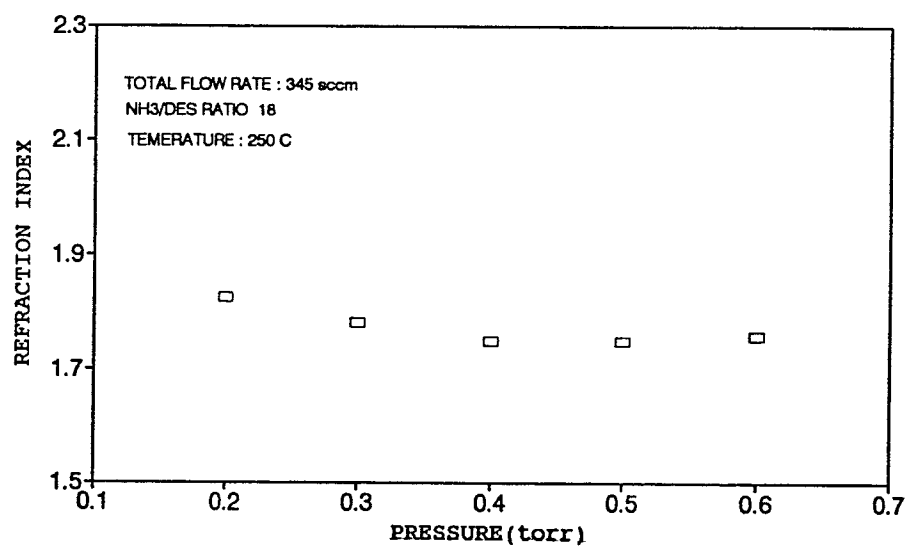


Figure 3.10 Effect of chamber pressure on refractive index.

shows Si/N ratio varied as NH₃/DES ratio increased. But a slight decrease in refractive index (n) corresponds to an increase in reactant ratio of NH₃/DES. We expect refractive index decrease with increasing NH₃/DES ratio. Figure 3.2 shows this trend, which generally observed.

3.2.2 The IR Spectra of Plasma Silicon Nitride Films

The IR spectra of plasma silicon nitride films shows a strong broad absorption around 890 cm⁻¹, which is due to the Si-N vibrations, and an absorption band at 3340 cm⁻¹ (N-H stretching) and 2170 cm⁻¹ (Si-H stretching). A typical IR spectrum is given in figure 3.11.

The IR spectra of the silicon nitride films deposited at different temperature were obtained. As the deposition temperature decreases, the hydrogen concentration increased, the absorption peak of Si-N shift from 890 to 900 cm⁻¹. This shift is in agreement with the standard plasma silicon nitride absorption peak(30). The N-H bonds in the film is formed preferably at the low frequency excitation of the plasma as suggested by Smith et al(31). The position of the Si-H absorption shifts to lower frequency as the N/Si ratio in the film decreases. Such a frequency shift for Si-H in Si₃N₄, SiO₂, amorphous Si, and phosphorus glasses has been analyzed by Lucovsky(32) and correlated with the electronegativity of the atoms or functional groups attached to the Si-H fragment. But, this analysis could not be applied to our SiNCO:H films as deposited because it is too restrictive.

All samples were examined by Infrared spectra and found two samples deposited at low temperature (100°C, 150°C) shows chemical composition unstable after deposition. In figure 3.12, the upper spectrum was done right after film was deposited, the lower spectrum in figure 3.12 was the result of IR analysis in one and half month later after deposition. As we can see in the figure 3.12, there was no Si-N bonding existing in the films deposited at 100°C, instead Si-O bonding appeared.

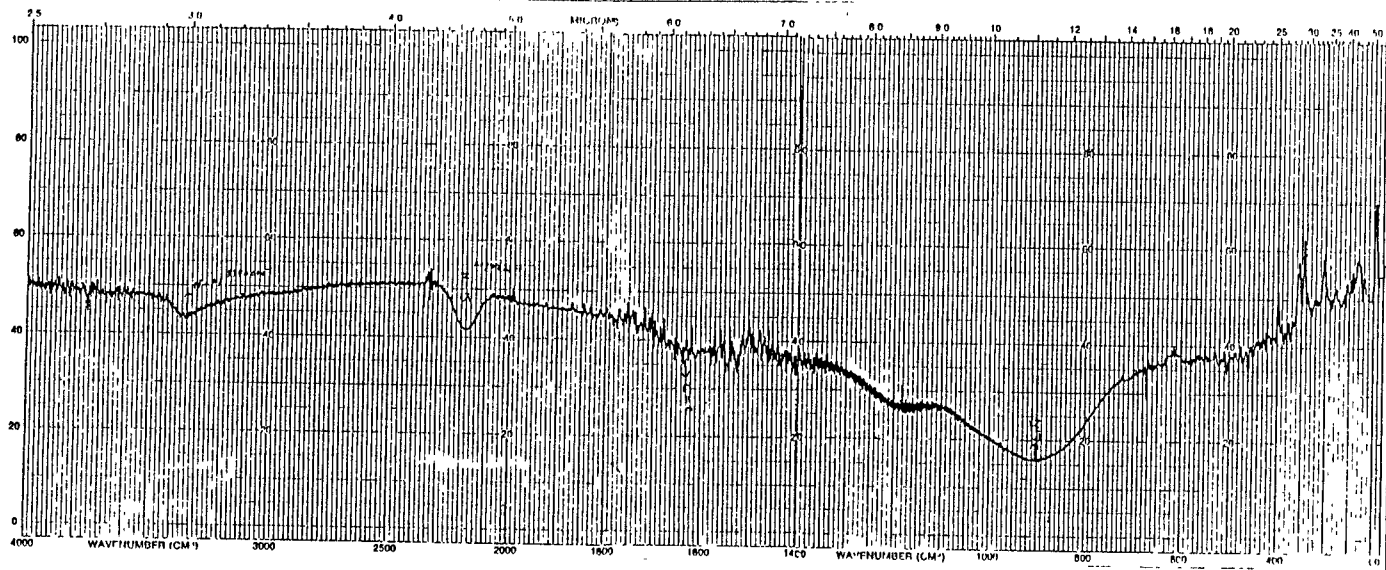


Figure 3.11 Infrared spectrum for the plasma deposited silicon nitride film.

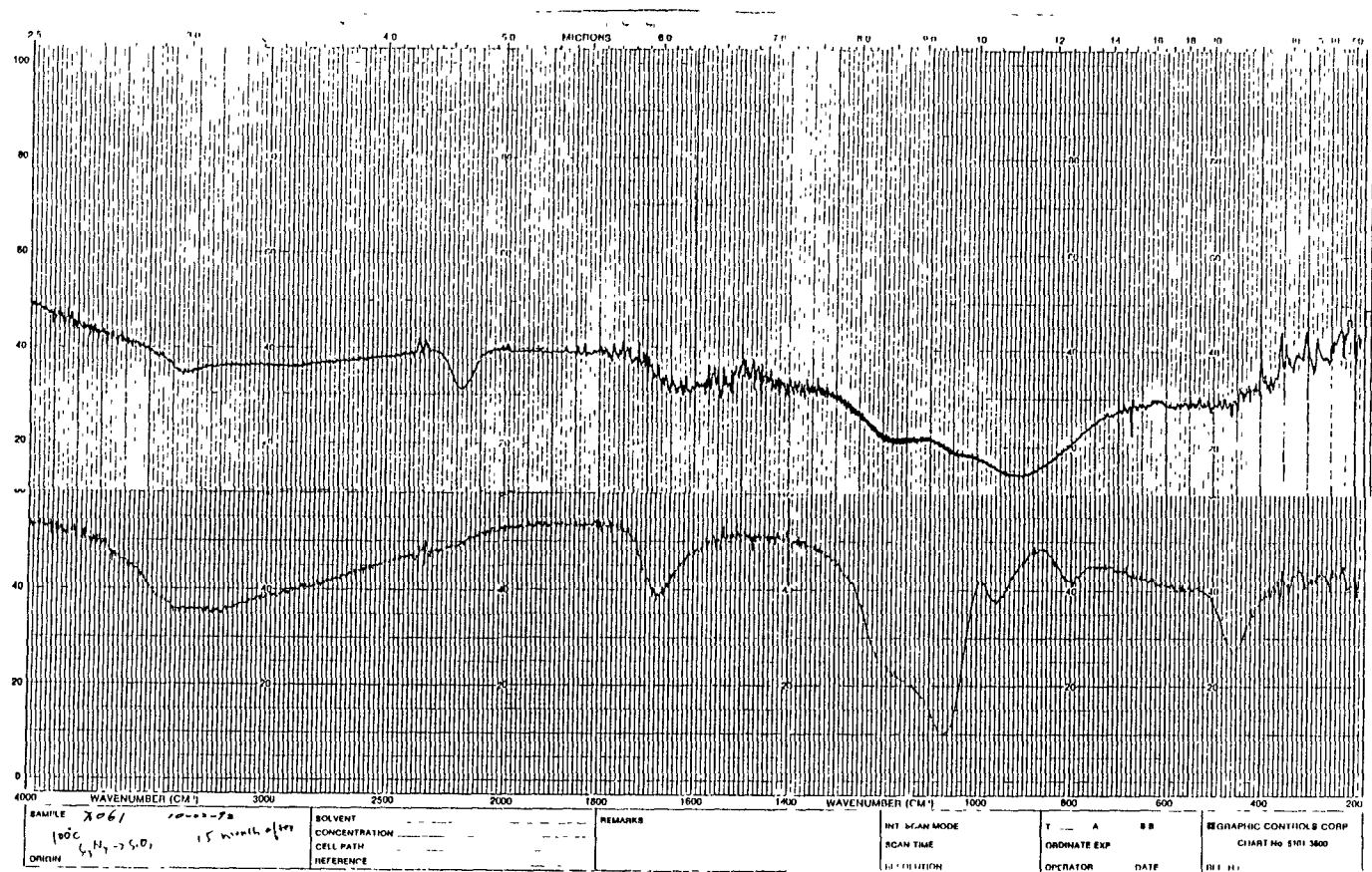


Figure 3.12 IR spectrum one month after deposition for the film deposited at 100 C.

The porous film deposited at low temperature containing a large concentration of incorporated hydrogen which may cause this problem.

3.2.3 The Effect of Heat Treatment on Film IR and Stress.

It is concluded from the IR spectra that the total hydrogen content of the films was seen to be reduced slightly with the heating at 450°C for 30 minutes. But this is not consistent with results of Tokunaga and Sugawara(33), who saw no loss of hydrogen in the heating of their films at 450°C for one hour. Figure 3.13 shows the spectra before and after heat treatment. The upper spectra in the figure 3.13 was done before annealing, and the lower one was done after annealing. The stress of the film changed to be less compressive from 415 MPa to 237 MPa after heat treatment. This is related to the total hydrogen content in the films. Also, this may be related to the movement of H from a N-H bond to an unsaturated Si bond. Pearce et al report that N-H₂ in PECVD is responsible for the compressive stress state in the film(34). The more detail about the effect of annealing on the film stress will be discussed on characterization section.

3.2.4 Deposition Uniformity of the Film

It is always desirable to maintain thin film thickness uniformity, it is absolutely essential for microelectronic and optical application. The thickness uniformity result showed that deposition rate decreases across the wafer, due to ammonia concentrating decreases radially along chamber radial position. There is about 10 percent deposition rate difference within a wafer. The figure 3.14 shows the deposition rate profiles as a function of position across wafer.

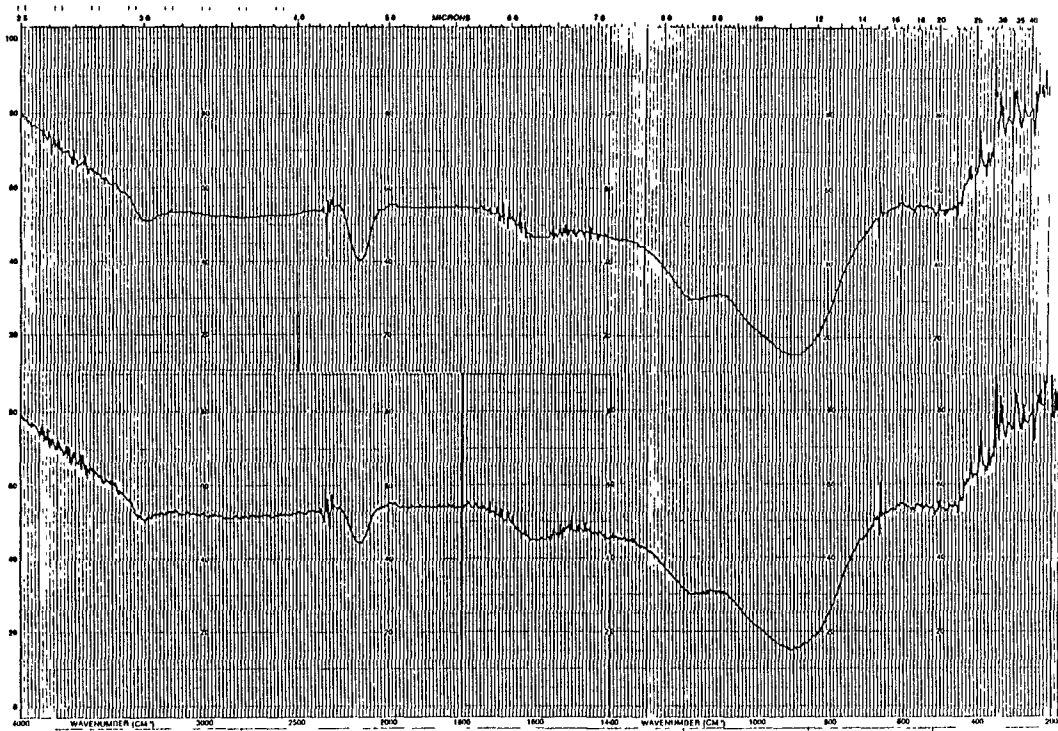


Figure 3.13 IR spectrum of silicon nitride before and after heat treatment

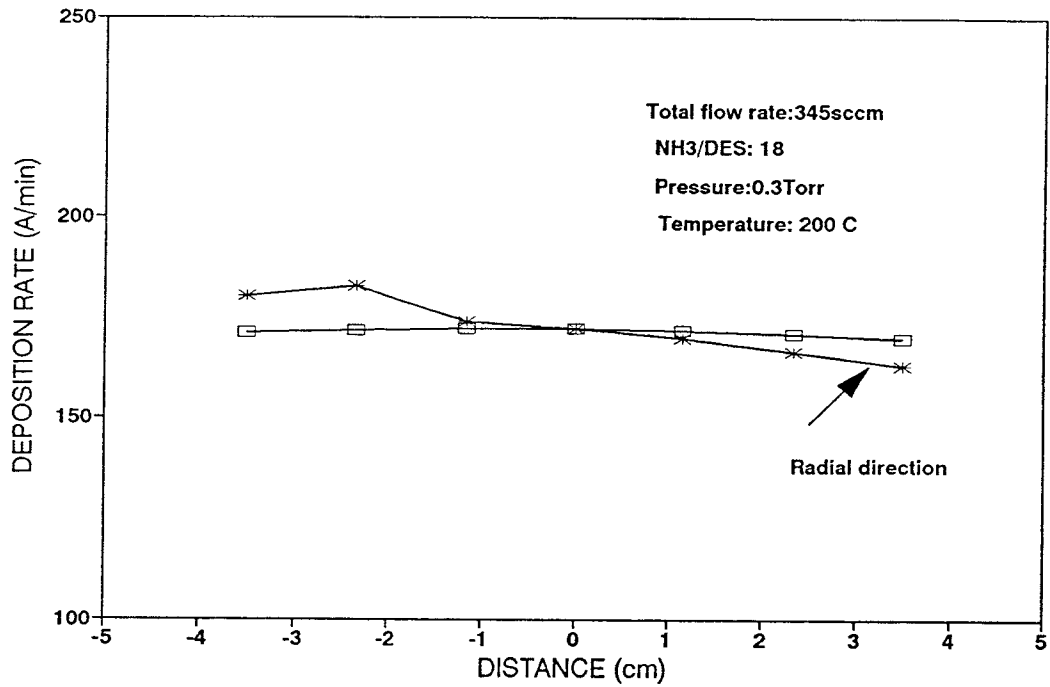


Figure 3.14 Deposition rate profiles as a function of radial position.

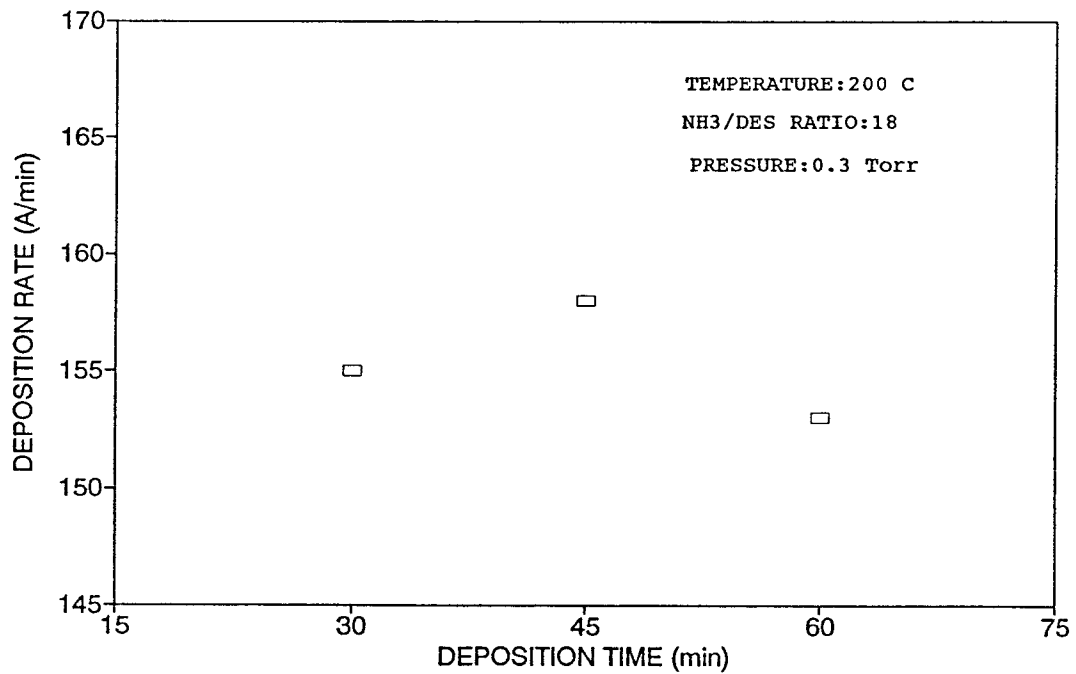


Figure 3.15 Effect of deposition time on deposition rate.

3.2.5 Effect of Deposition Time on Deposition Rate

At a constant power, an increase in the deposition time brought a slight reduction in the effective deposition rate of plasma silicon nitride. The substrate temperature slightly increased with passage of time due to ion bombardment to substrate surface. As discussed above it results deposition rate slight decrease. A plot of deposition rate vs. deposition time is shown in figure 3.15.

3.2.6 Optical Transparency Result

The silicon nitride films deposited on plain glass has been measured in the UV region (200-800 nm wavelength) for optical transmission. The absorption coefficient, a , was calculated by using equation $I/I_0 = \exp(-at)$, where I/I_0 is the percent transmittance, t is the film thickness. The wavelength of 620 nm was considered to represent absorption. All silicon nitride samples show high transparency. Figure 3.16 shows a typical absorption diagram.

3.3 The Characterization of the Films

3.3.1 Mechanical Stress Measurement

The mechanical stress in the silicon substrate/film system related the film thickness and the substrate manifests itself in the form of bending. The stress is measured by home-made system, which uses two He-Ne laser beams. Figure 2.1 is a optical imaging system for setup.

The mechanical stress can be determined by the formula given below(35):

$$\sigma = \frac{E t_s^2}{6(1-\nu) R t}$$

where E = Young's modulus for the substrate,

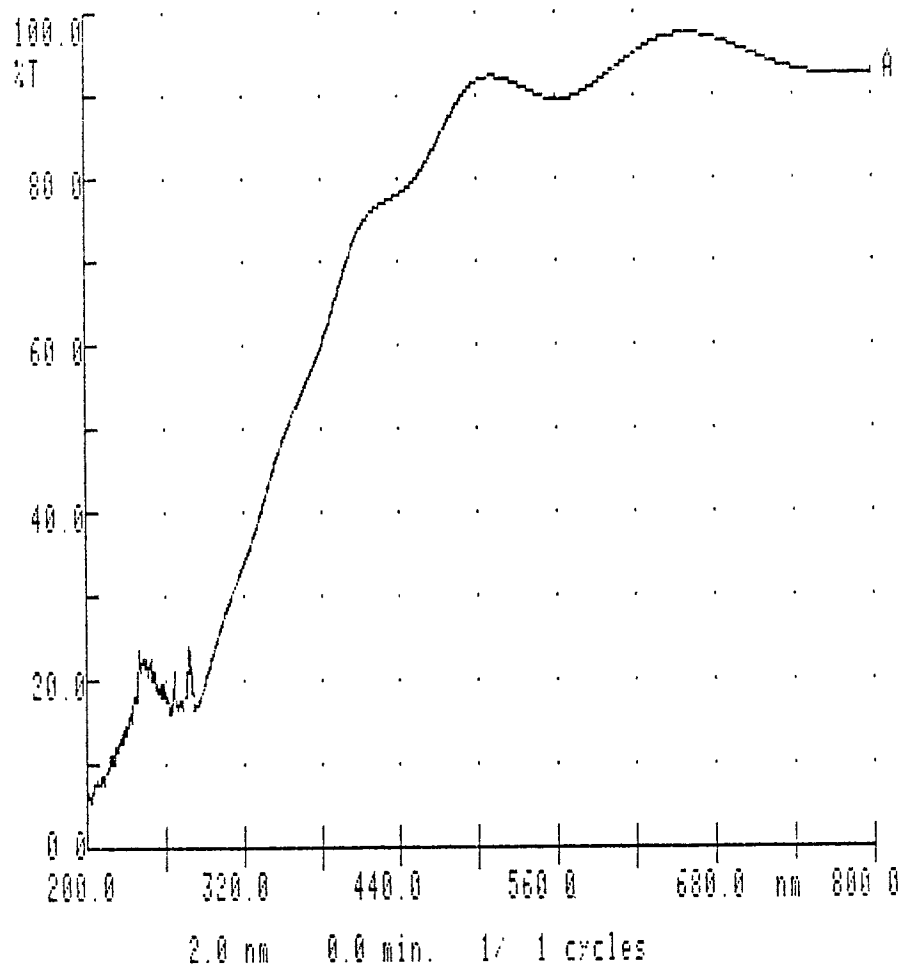


Figure 3.16 A typical optical transmission diagram.

τ = Poisson ratio for the substrate,

t_s = thickness of the substrate,

t = thickness of the film,

R = net radius of curvature.

R , the radius of curvature is calculated from following formula:

$$R = 1 / (1/R_2 - 1/R_1)$$

where R_1 = the radius of curvature of the wafer before deposition

R_2 = the radius of curvature of the wafer after deposition.

For Si <100>, $E/(1-\tau) = 1.8 \times 10^{11}$ Pa. Wafers with a thickness of about 525 μm were used for stress measurement.

Thus, for the system used in this experiment, a simple formula is produced:

$$\sigma = 12.4 \times \frac{d \text{ (mm)}}{t_f \text{ (m)}} \text{ (Pa) (see appendix 2)}$$

Where d = the distance change on the screen before and after deposition, and t_f = film thickness.

All as-deposited films were found to have a compressive stress. Table 3.2 lists all experiment stress results. From the literature it is unknown that even tensile silicon nitride films become compressive when they are exposed to ion bombardment(36). This is explained by an expansion of the layer due to implanted atoms and broken Si-N bonds, resulting in film expansion. The stress behavior is related to hydrogen content, ion bombardment and other impurities such as carbon. Generally, the hydrogen desorption is controlled by thermal and ion bombardment. As discussed before, hydrogen desorption can be enhanced by increasing the deposition temperature, or at lower frequencies by ion bombardment. The influence of ion bombardment on the hydrogen desorption can be assumed to independ of the deposition temperature. Thus, the hydrogen content in the layer is determined by ion bombardment at low temperature while at high temperature this content is

determined by thermal desorption. For deposition condition of this study the hydrogen desorption rate is controlled by thermal and ion bombardment.

The stress in the films seems to have more compressive as deposition temperature increases. Hence, for our study, in this temperature range, the film with lowest hydrogen has the largest compressive. A very similar stress behavior has been observed by other investigators(25), and found for silicon-oxynitride films(37).

As we know a relatively high temperature anneal will lead to hydrogen desorption. This will result in a densification and shrinkage of the film, which will shift the stress behavior toward less compressive (or tensile) type character. The annealing experiment have demonstrated this result. If the stress in the layers is too high, the film induces defects in the substrate material or tends to peel off. High tensile stress cause cracking of the film. Hence, low compressive stress is usually preferred.

3.3.2 The Hardness and Young's Modulus Measurement

The hardness and Young's modulus of thin layers have been measured by nanoindenter. Schematic diagram of the indenting mechanism of the Nano-indenter is given in figure 2.2. To calculate the hardness and modulus of the films the plastic depth must be determined. The hardness is obtain by using formula:

$$H = P / A$$

where P is the applied load and A is the contact area calculated from the known geometry of the indenter:

$$A = 24.56 h_p^2 + 225.94 h_p^{3/2} + 519.61 h_p$$

where h_p is plastic depth.

Assuming that the area in contact remains constant during initial unloading and adopting the solution of Sneddon(38) for the elastic deformation of an isotropic

elastic material with a flat-ended cylindrical punch, the elastic modulus is obtained from the contact stiffness S , the slope of the unloading curve, given by:

$$S = dP / dh = 2 E_T (A/\pi)^{1/2}$$

where h is the displacement of the indenter, and E_r is the composite modulus for the indenter-sample combination.

$$E_r = [(1-r_f^2)/E_f + (1-r_i^2)/E_i]^{-1}$$

where E_f and E_i are Young's moduli for film and indenter respectively, and r_f and r_i are poisson's ratios for film and indenter respectively. Since r appears as a quadratic term and therefore represents only a small correction, we took $r_f = 0.3$ for the calculation, and for diamond indenter E_i and r_i are 1010 GPa and 0.213 respectively.

The following experimental conditions were used: the maximum drift rate prior to testing = 0.1 nm/s, the loading rate = 200 μ N/sec to a maximum load of 4.5 mN, the hold time = 1 minute, and temperature = 21°C. Sixteen indents were performed on every sample.

Figure 3.17 - 3.18 presents the Young's modulus and hardness with error bar, as function of deposition temperature (100°C - 300°C) at constant NH_3/DES ratio 18 and chamber pressure 0.3 torr. High deposition temperature leads to a increase of hardness and Young's modulus. After the deposition temperature is over 200°C, the increasing rate slows down. For the constant conditions of temperature (250°C) and pressure (0.3 torr), the increase in ammonia flow rate had the effect of increasing the Young's modulus. This can be explained by saying that the more nitride in the film the higher Young's modulus, and related to bonding energy. Figure 3.19 - 3.22 shows both the Young's modulus and hardness at different ammonia/DES ratio (for both deposition in a N_2 atmosphere and with no N_2). The Young's modulus and hardness for pressure set varied little as a function of pressure.

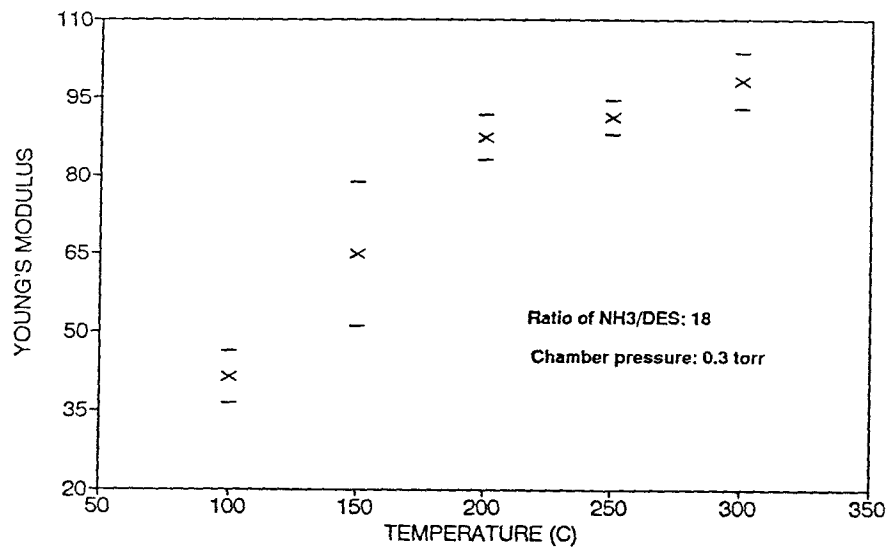


Figure 3.17 Effect of substrate temperature on Young's modulus.

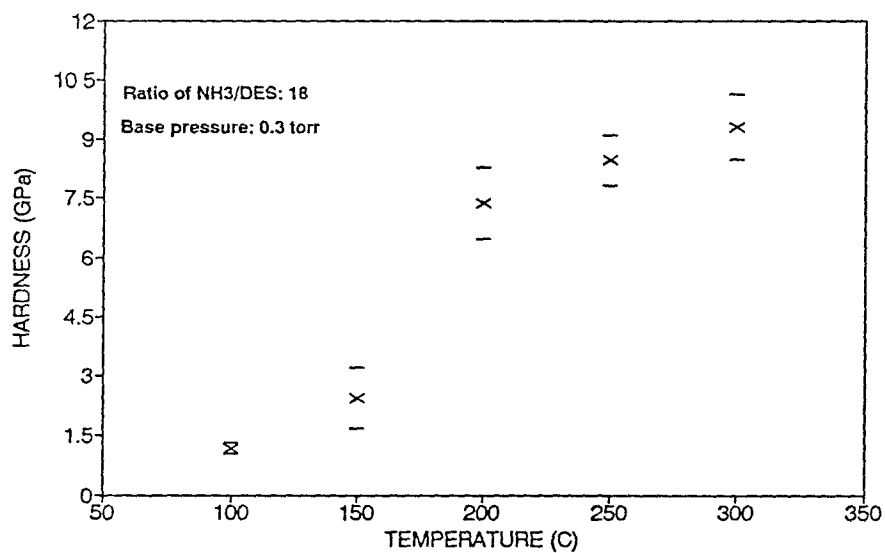


Figure 3.18 Effect of substrate temperature on hardness.

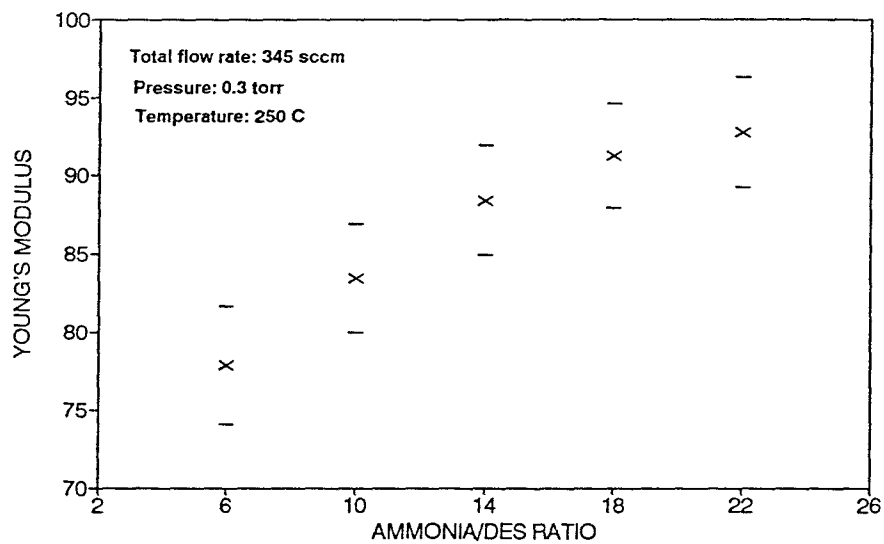


Figure 3.19 Effect of NH_3 /DES ratio on Young's modulus.

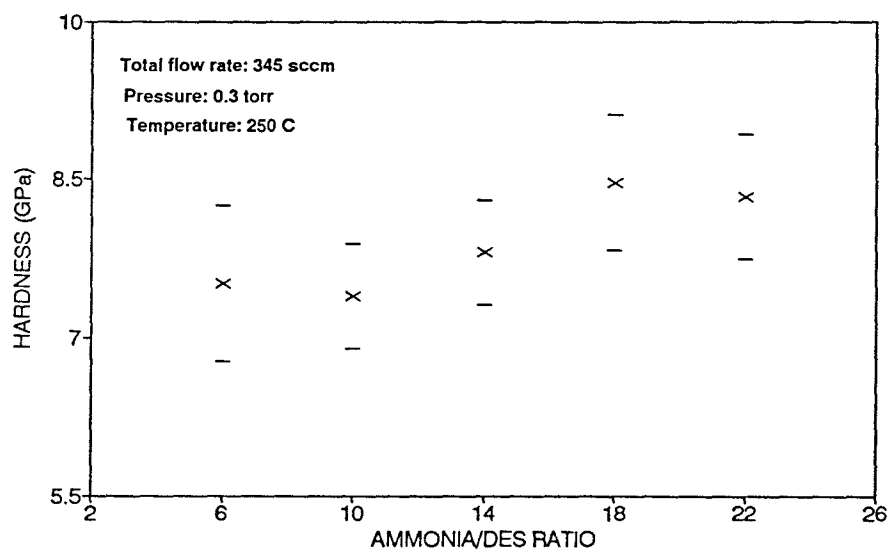


Figure 3.20 Effect of NH_3 /DES ratio on hardness.

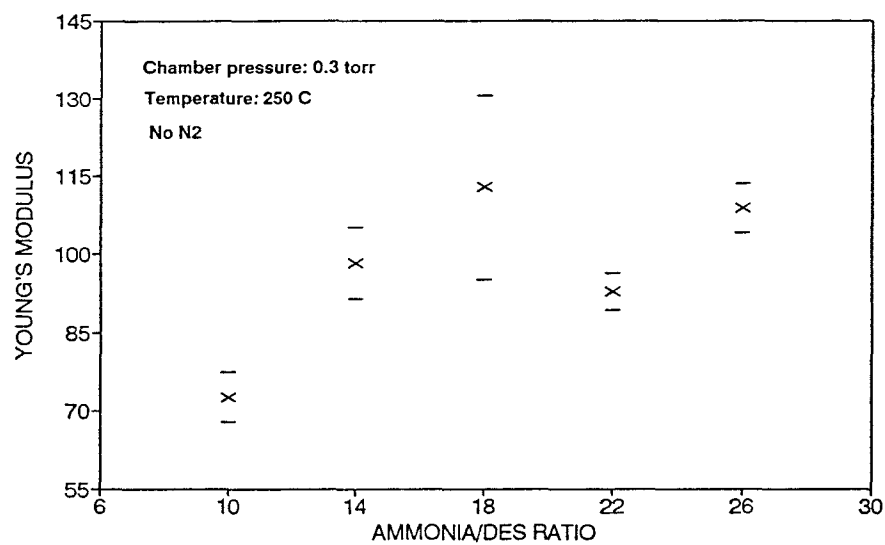


Figure 3.21 Effect of NH₃/DES ratio on Young's modulus with no N₂.

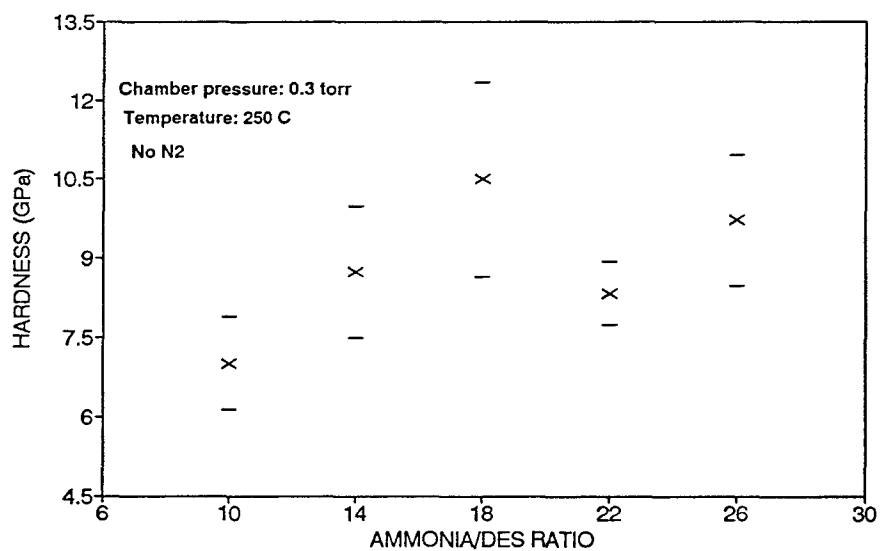


Figure 3.22 Effect of NH₃/DES ratio on hardness with no N₂

CHAPTER 4

CONCLUSION

Silicon nitride thin films were deposited on silicon wafers and plain glass slides by plasma enhanced chemical vapor deposition using diethylsilane (DES) and ammonia, at a temperature range of 100°C - 300°C, a pressure range of 0.2 - 0.6 torr, and NH₃/DES ratio of 6 - 26. The DES flow rate was fixed at 15 sccm. These films were found to have compressive mechanical stress and high optical transparency.

All silicon nitride films as deposited had a large concentration of carbon. The composition of the samples deposited in N₂ atmospheres were very similar. The carbon is about 70% SiC and 30% free carbon for the ratio set experiments with N₂ gas. The carbon composition of the samples deposited without N₂ gas was present more as free carbon, in the range between 55/45 to 60/40 free carbon/carbide. The deposition rate was found to be inversely proportional to the deposition temperature and to the NH₃/DES ratio, but proportional to the chamber pressure. The increase in NH₃/DES ratio has the effect of increasing the Young's modulus and hardness. The heat-treatment at 450°C for half hour lead to a densification of the film and results in films that are less compressive.

APPENDIX A
PHYSICAL PROPERTIES OF DIETHYLSILANE (DES)

Chemical formula: $(C_2H_5)_2SiH_2$

Molecular weight: 88.2

Normal Boiling point: $56^{\circ}C$

Density: 0.6843 g/cm^3

Appearance: colorless liquid

Vapor pressure * : 200 torr at $25^{\circ}C$

Freezing point: $<-76^{\circ}C$

Solubility in H_2O : insoluble

Flash point: $-20^{\circ}C$ (closed cup)

Autoignition temperature: $218^{\circ}C$

* vapor pressure data:

$$\ln p = 17.4741 - 3569.1 / T (^{\circ}C), \text{ pressure in torr}$$

APPENDIX B

THE PRINCIPLE OF THE OPTICAL IMAGING METHOD

The development of the theory for stress is based on the work done by Stoney which actually laid the foundation of experimental analysis of stress. The experimental optical setup is shown in figure 2.1. The image distortion produced by a warped surface is schematically shown in figure B.1, which shows that two beams A and B (with a small divergence of 2β) incident at positions W_1 and W_2 will reflect and form a magnified image I_1I_2 in the image plane. For the convex surface, the image formed is $I'_1I'_2$. From geometry, the size of the image is

$$I_1I_2 = W_1W_2 + 2L \tan \beta \quad (1)$$

and
$$I'_1I'_2 = W_1W_2 + 2L \tan(\beta + 2\Theta) \quad (2)$$

where L = the distance between the image plane and the wafer surface, and 2Θ is the angle of bending for the convex wafer. The image distortion due to the convex surface is

$$d = I'_1I'_2 - I_1I_2 = 2L (2\Theta) \quad (3)$$

for small Θ and β .

$$2\Theta = d / 2L \quad (4)$$

The magnification factor m , defined as the ratio of reference image I_1I_2 and reference spacing W_1W_2 , $m = I_1I_2 / W_1W_2$ can be obtained from equation (1) above.

The radius of curvature is

$$R = \frac{\text{arc } W_1W_2}{2\Theta} = 2L (I_1I_2) / md \quad (5)$$

When the m is taken in equation (5),

$$R = \frac{W_1W_2}{d / 2L} \quad (6)$$

For the stress measurement system used in this experiment, $2L = 9954$ mm and $W1W2 = 62$ mm, and d is measured from the screen. Stress is calculated from the formula:

$$\sigma = \frac{E}{6(1-\nu)} \frac{t_s^2}{Rt} = 12.4 \times \frac{d \text{ (mm)}}{t_f \text{ (m)}} \text{ (Pa)}$$

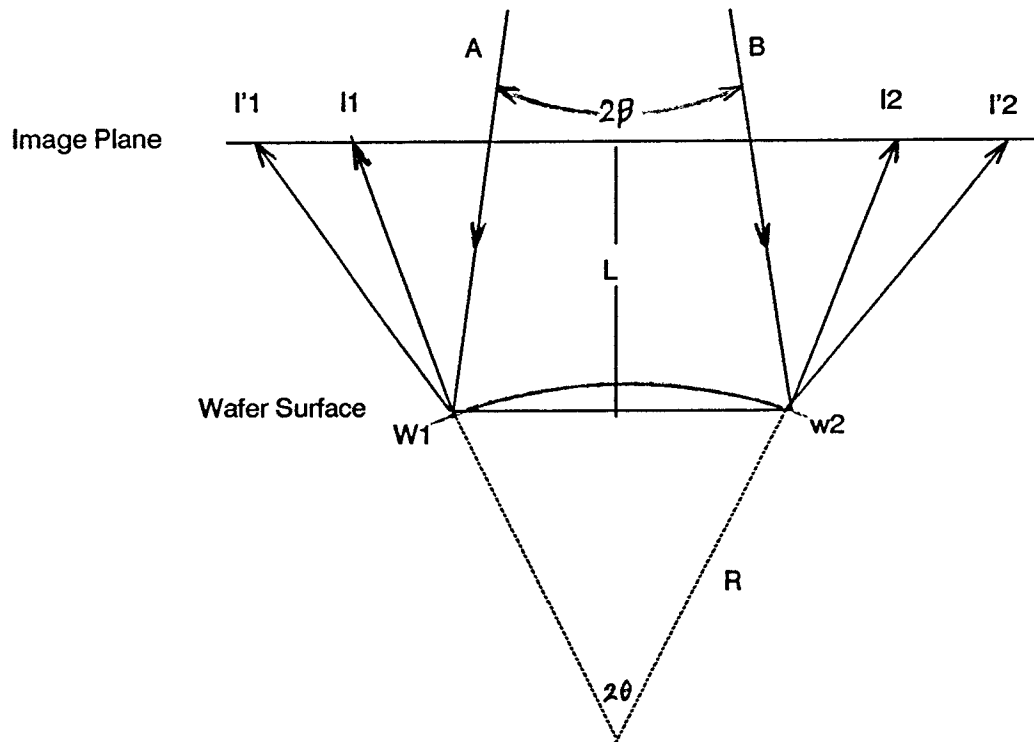


Figure B.1 The principle of the optical imaging method.

APPENDIX C

DEPOSITION PROCEDURE

Perform to load substrate as follows:

- 1). Set DEPOSITION model. Select AUTO/MAN switch to the AUTO position. Set deposition timer (DEPOSIT TIME) to the desired level. Turn on the cooling water, open the nitrogen tank valve.
- 2). At the engineering control panel, set the status at back-fill stage by pressing ADVANCE button. Turn on the nitrogen flow switch.
- 3). The alarm is on and the COMPLETE status light is on when the chamber is opened. Press ALARM SILENCE button.
- 4). Load the substrates.
- 5). Manually hold the lid down, then press the START button. The system will pump down to a low pressure. Press STOP button to make PUMP DOWN status.
- 6). Set deposition temperature at temperature controller, turn on the heater. wait for one hour. Apply electrical power to DES flow controller.

To start deposition as follows:

- 7). Open ammonia tank valve. Set desired ammonia flow rate at engineering panel.
- 8). Turn on R. F. power supply.
- 9). Press START button, the START light is on. The system will pump to a low pressure. Turn on the booster-pump. the system will pump down to 0.01 torr.
- 10). Once the system is at base pressure (0.01 torr), it will go to next status HIGH PURGE. At this stage, the high flow nitrogen backfill and the subsequent pump down to 0.01 torr.
- 11). Then, the system will be PRE PURGE status automatically. During this stage, the nitrogen pre purge.

- 12). Turn on DES vapor flow, when the PROC GAS status is on. Adjust nitrogen flow rate to the desired level. At this stage, the system will reach the pressure which is set.
- 13). After deposit pressure is maintained for about 30 seconds, a signal to turn on RF power supply is sent, and the VOLTS status light comes on.
- 14). The system now advances to DEPOSIT status, and countdown of the deposit timer on the engineering control panel starts. (At this point, the following status lights will be on DEPOSIT, PROC GAS, N₂, NH₃, PRESS (torr), VOLTS, AMPS, KILOWATTS AND DEPOSIT MODE).
- 15). When the deposit timer reaches zero, the POST-URGE status light is on, nitrogen flow continues to flow for 30 seconds.
- 16). After post-purge the reactor is pumped down to base pressure. Press STOP button, the system goes to PUMP DOWN status.
- 17). Turn off heater. Leave it for five hours to cool down with cooling water.
- 18). To take substrate out is same means as load substrate. Check the system.

REFERENCES

1. W. A. P. Claassen, W. G. J. N. Valkenburg, F. H. P. M. Habraken, *J. Electrochem. Soc.*, **130**, 2419(1983).
2. C. Blaauw, *J. Electrochem. Soc.*, **131**, 1114(1984).
3. S. V. Nguyen, S. Fridman, *J. Electrochem. Soc.*, **134**, 2324(1987).
4. B. R. Soller, C. R. Snider, R. F. Shuman, *J. Electromech. Soc.*, **131**, 868(1984).
5. D. C. Bartle, D. C. Andrews, J. D. Grange, *Vacuum*, **34**, 315(1984).
6. S. K. Ray, C. K. Maiti, N. B. Chakrabarti, *J. Electroic Materials*, **20**, 907(1991).
7. J. N. Chiang, D. W. Hess, *J. Appl. Phys.*, **67**, 685(1990).
8. G. J. Valco, V. J. Kapoor, M. D. Biedenbender, *J. Electrochem. Soc.* **136**, 175(1989).
9. K. Tokunaga, K. Sugawara, *J. Electrochem. Soc.*, **138**, 176(1991).
10. E. P. G. T. Van de Ven, *Solid State Tech.*, **24**, 167(1980).
11. John Yuan-tai Chen, Richard C. Henderson, James T. Hall and John W. Peters *J. Electrochem. Soc.*, **131**, 2146 (1984).
12. S. M. Sze, Semiconductor Devices Physics and Technology, p360, John Willey and Sons, New York, 1985.
13. M. Maeda and H. Nakamura, *Thin Solid Films*, **112**, 279 (1984).
14. K. Suzuki, J. Matsui, and T. Torikai, *J. Vac. Sci. Tech.*, **20**, 191 (1982).
15. D. C. Bartle, D. C. Andrews, J. D. Grange, P. G. Harris, A. D. Trigg, and D. K. Wickenden, *Vacuum*, **34**, 315 (1984).
16. R. Hezel and R. Schorner, *J. Appl. Phys.*, **52**, 3076 (1981).
17. H. Watanabe, K. Katoh, and M. Yasui, *Jap. J. Appl. Phys.*, **23**, 1 (1984).
18. J. T. Milek (ed.), Handbook of Electronic Materials, Vol.6, Silicon Nitride for Microelectronic Applications, Part II, Plenum, New York, 1972.
19. Klaus K. Schuegraf (ed.), Handbook of Thin Film Deposition Processes and Techniques, p302, Noyes Publications, Park Ridge, 1988.
20. W. Kern and G. L. Schnable, *IEEE Trans. Electron Devices*, **ED-26**, 647 (1979).
21. R. G. Rieser, *J. Electrochem. Soc.*, **115**, 1092(1968).
22. W. Wada and M. Ashikawa, *Jpn. J. Appl. Phys.*, **51**, 1725(1976).

23. R. A. Levy, Microelectronic Materials and Processes, p214, Kluwer Academic Publishers, Dordrecht, The Netherlands, 1989.
24. John L. Vossen and Werner Kern, Thin Film Processes, Academic Press, Orlando, 1978.
25. W. A. P. Classen, W. G. J. N. Valkenburg, M. F. C. Willemsen, and W. M. v. d. Wijgert, J. Electrochem. Soc., **132**, 893(1985).
26. B. Drevillion, J. Huc, A. Lloret, J. Perrin, Appl. Phys. Lett., **37**, 646(1980).
27. R. H. Bruce, J. Appl. Phys., **52**, 7064(1981).
28. G. Turban, Y. Catherine, and B. Grolleau, Thin Solid Films, **67**, 309(1980).
29. A. K. Sinha, H. J. Levinstein, T. E. Smith, G. Quintana, and S. E. Haszko, J. Electrochem. Soc., **125**, 601(1978).
30. W. R. Knolle and J. W. Osenbach, J. Appl. Phys., **58**, 1248(1985).
31. Donald L. Smith, Andrew S. Alimonda, J. Electrochem. Soc., **137**, 614(1990).
32. G. Lucovsky, J. Vac. Sci. Tech., **16**, 1225 (1979).
33. K. Tokunaga and Sugawara, J. Electrochem. Soc., **138**, 176(1991).
34. C. W. Pearce, R. F. Fetcho, M. D. Gross, J. Appl. Phys., **71**, 1838(1992).
35. J. Kanicki, Mater. Res. Soc. Symp. Proc., **118**, 671(1988).
36. E. P. Eernisse. J. Appl. Phys., **48**, 3337(1977).
37. W. A. P. Classen, H. A. J. Th. v. d. Pol, and A. H. Goemans, J. Electrochem Soc., **133**, 1458(1986).
38. I. E. Sneddon, Int. J. Eng. Sci., **3**, 47 (1965).